



CHALMERS
UNIVERSITY OF TECHNOLOGY



Quantifying the environmental impacts of braking emissions

Ideal brake pad materials for a sustainable future

PAVANKUMAR KULKARNI
ELSA MARIE KENDRICK

Department of Industrial and Materials Science
Division of Materials and Manufacture
CHALMERS UNIVERSITY OF TECHNOLOGY
Gothenburg, Sweden 2021

MASTER'S THESIS 2021

Quantifying the environmental impacts of braking emissions

**PAVANKUMAR KULKARNI
ELSA MARIE KENDRICK**

**Examiner, Chalmers: Mats Norell
Supervisors, Volvo Cars: Quintus Jalkler and Staffan Johansson**

**Department of Industrial and Materials Science
Division of Materials and Manufacture
CHALMERS UNIVERSITY OF TECHNOLOGY
Gothenburg, Sweden 2021**

Quantifying the environmental impacts of braking emissions

Ideal brake pad materials for a sustainable future

PAVANKUMAR KULKARNI

ELSA MARIE KENDRICK

© PAVANKUMAR KULKARNI & ELSA MARIE KENDRICK, 2021

Master Thesis 2021 for Pavankumar Kulkarni

Department of Industrial and Materials Science
Division of Materials and Manufacture
Chalmers University of Technology
SE-412 96 Gothenburg, Sweden
Telephone: + 46 (0)31-772 1000

Cover:

Brake pad surface on the cover is captured under a scanning electron microscope during the thesis

Chalmers digitaltryck
Gothenburg, Sweden 2021

1 Abstract

This work compares particle emissions coming from three different brake pad materials in order to determine which material produces the least emissions, and two different braking cycles in order to analyze the effect of electrification in the automotive industry on braking particle emissions due to regenerative braking.

The targeted market for this research is the European market, and therefore Volvo's European brake pads (ECE) were treated as the baseline material tested with a gray cast iron brake disc and the WLTP (Worldwide Harmonized Light Duty Vehicles Test Procedure) braking cycle for ICE (internal combustion engine) vehicles. This test procedure was repeated for two other brake pads: non-asbestos organic (NAO) commonly used in USA and Asian markets, and a new composition of non-asbestos organic produced by Volvo's supplier (new NAO) to mitigate brake emissions. Then the test procedure was repeated for ECE brake pads with a modified WLTP braking cycle to simulate the decrease in magnitude of friction braking with an electric vehicle. Tests were done using a closed-chamber brake dynamometer and an electrostatic precipitator for particle mass and count measurements in real time. A membrane-type filter made by Pallflex was used for particle collection.

This study found that a majority of the particles measured were less than $1\mu\text{m}$ in diameter (PM₁), and that of the four experiments considered, ECE brake pads produce the most braking emissions in terms of both mass and count. The second highest quantity of emissions emitted came from the NAO brake pads in terms of both mass and count. Then, the new NAO pads and ECE pads with the EV braking cycle produced the least amount of emissions, new NAO producing the least emissions by mass, and ECE EV braking cycle producing the least emissions by count.



Contents

1	Abstract	1
2	List of Acronyms	5
3	Preface	6
4	Introduction	7
5	Braking Systems	8
5.1	Friction Braking	8
5.1.1	Friction Braking System Overview	8
5.1.2	Friction Braking Performance Parameters	9
5.2	Regenerative Braking	10
6	What Are Braking Emissions?	11
6.1	Environmental and Health Concerns	11
6.2	Proposed Legislation for Non-Exhaust PM Emissions	13
6.3	Capturing and Measuring Braking Emissions	14
6.3.1	Case Studies	14
6.3.2	Summary: Moving Forward	15
7	Electrification in the Automotive Industry and Impact on Braking Emissions	16
7.1	The Future of Braking Systems and Braking Emissions	16
7.2	Future EV Impact on Braking Emissions	16
7.3	Projection for Braking Emissions	18
8	Brake Disc and Brake Pad Materials	22
8.1	Brake Pad Materials (Friction Materials)	22
8.1.1	Abrasives	23
8.1.2	Friction Modifiers	23
8.1.3	Reinforcements/Fibers	24
8.1.4	Binders	25
8.1.5	Classification of Brake Pads	25
8.2	Brake Disc Materials	26
8.2.1	Cast Iron	27
8.2.2	Aluminum Composites	27
8.2.3	Ceramics	28
9	Material Wear Mechanisms	30
9.1	Classification of wear	30
9.2	Brake Pad Wear	31
9.2.1	Formation of Friction layer	31
9.2.2	Development of Contact Plateau	31
9.2.3	Wear	32
10	Methodology	33
10.1	Test Setup	33
10.1.1	Overview	33



10.1.2 Brake Dynamometer	34
10.1.3 Electrostatic Precipitation Particle Measurement	34
10.1.4 Particle Capture Equipment	36
10.2 Dynamometer Test Cycles	36
10.3 Experimental Test Plan	38
10.4 Ranking Parameters To Be Measured	38
11 Results	40
11.1 PM Emissions	40
11.2 Brake Disc Temperature	43
11.3 Wear Measurements	44
11.3.1 Thickness and Weight Measurements	44
11.3.2 Flatness Profile Measurements	46
11.4 Scanning Electron Microscopy (SEM) and Energy dispersion spectrum (EDS) analysis	47
11.4.1 Filter analysis	47
11.4.2 Brake Pad Analysis	49
12 Discussion	52
12.1 PM Emissions Comparison Between Brake Pad Materials	52
12.2 PM Emissions Comparison Between Braking Cycles	53
12.3 PM Emissions Overview	55
12.4 Material Wear Comparison Between Brake Pad Materials	56
12.4.1 Amount of Wear	56
12.4.2 Nature of Wear	57
12.4.3 Elemental Analysis of Brake Pad Surface	60
12.5 Best Brake Pad Candidate for Reduced Environmental and Human Impact	60
13 Conclusion	61
14 Future Work & Recommendations	62
References	63



List of Figures

5.1	Side Profile of Disc Brake [1]	8
5.2	Regenerative Braking Map in an Electric Vehicle [2]	10
7.1	Brake Blending Between Friction Braking and Regenerative Braking [3]	17
7.2	Disc Temperature and Brake Pressure for ICE vs. EV [3]	18
7.3	Road Transport PM2.5 Emissions Sources by Year in United Kingdom [4]	19
7.4	Predicted PM2.5 Levels due to Exhaust vs. Non-Exhaust Sources until 2030 in United Kingdom [4]	20
7.5	Global Increase in Electric Vehicle Fleet vs. ICE Fleet [5]	21
10.1	Side View of Brake Dyno Test Setup	33
10.2	Front View of Brake Dyno Test Setup	34
10.3	Flow Meter Test Locations in the Dyno Test Chamber	35
10.4	Burnishing Cycle Speed Profile	36
10.5	WLTP Novel Brake Cycle Speed Profile	37
11.1	ECE Pads Linear Driving Speed Profile vs. PM Emissions	40
11.2	NAO Pads Linear Driving Speed Profile vs. PM Emissions	41
11.3	New NAO Pads Linear Driving Speed Profile vs. PM Emissions	42
11.4	ECE Pads with EV Cycle Linear Driving Speed Profile vs. PM Emissions	42
11.5	Average Disc Temperature in 1-minute Intervals vs. PM Emissions for ECE Pads	43
11.6	Flatness profile measurements for ECE pads tested with WLTP ICE	46
11.7	Flatness profile measurements for NAO pads tested with WLTP ICE	47
11.8	Filters for 4 tests after particle collection	48
12.1	Average Particle Mass in $\mu\text{g}/\text{m}^3$ Measured During WLTP Cycle for Different Brake Pad Materials	52
12.2	Average Particle Count in $\#/\text{cm}^3$ Measured During WLTP Cycle for Different Brake Pad Materials	53
12.3	Average Particle Mass in $\mu\text{g}/\text{m}^3$ Measured During WLTP Cycle for ICE vs. EV	54
12.4	Average Particle Count in $\#/\text{cm}^3$ Measured During WLTP Cycle for ICE vs. EV	54
12.5	Average Particle Mass in $\mu\text{g}/\text{m}^3$ Overall Comparison Between Materials and Braking Cycles	55
12.6	Average Particle Count in $\#/\text{cm}^3$ Overall Comparison Between Materials and Braking Cycles	56
12.7	Adhesive friction on ECE pads (ICE cycle)	57
12.8	Secondary plateau failure in ECE pads (EV cycle)	57
12.9	Piston location on inner pads	58
12.10	Piston location on outer pads)	58
12.11	ECE pads	58
12.12	NAO pads	58
12.13	New NAO pads	58
12.14	3D surface topography of new ECE pad	59
12.15	3D surface topography of worn ECE pad	59
12.16	Sliding direction on the pad	59
12.17	Measuring direction on the pad	59



2 List of Acronyms

Acronym	Meaning
ICE	internal combustion engine
EV	electric vehicle
PM	particulate matter
ECE	ECE-R90 brake regulation for Europe
NAO	non-asbestos organic
dyno	dynamometer
ESP	electrostatic precipitator
GCI	gray cast iron
WLTP	Worldwide Harmonized Light Duty Vehicles Test Procedure
LACT	Los Angeles City Traffic
EDS	energy dispersive spectroscopy
Al MMC	aluminum metal matrix composites
VCC	Volvo Cars Corporation
HEPA	high efficiency particulate air

3 Preface

This thesis was conducted by Pavankumar Kulkarni of Chalmers University of Technology in Gothenburg Sweden, in the Department of Industrial and Material Science and Elsa Kendrick of the Polytechnic University of Catalonia in the Department of Industrial Engineering. Both students participated in the Volvo Engineering Student Concept Program at Volvo Cars, meaning they worked at Volvo Cars during the summer between the first and second years of their respective master's programs, and were welcomed back to conduct a master thesis. Though they belonged to different background, they combined knowledge to produce a well-rounded master thesis regarding braking particle emissions

Elsa focused on the study of the test setup and how to quantify the braking emissions, as well as the electric vehicle and internal combustion engine braking cycles. Pavankumar focused on the material analysis of the friction materials before and after testing. Both having a background in mechanical engineering, but Elsa's master program focusing in energy engineering, and Pavankumar's in material science engineering, they combined knowledge to produce a well-rounded master thesis regarding braking particle emissions. This report published at Chalmers University of Technology serves as master thesis for Pavankumar Kulkarni



4 Introduction

High levels of particulate matter (PM) in the air have proven to be dangerous for the environment and human health, particularly in urban areas. Depending on the size, shape, and elemental composition of these fine airborne particles, they can cause problems for respiratory health, contribute to smog, and even negatively affect water resources [6]. For this reason, there have been many studies done on what human activities contribute to the levels of these small particles in ambient air. Without a doubt, one of the main contributors to particulate matter levels is the transport industry, and particularly road transport, which contributes 30% of all particulate matter emissions [7]. And for the past decades, exhaust emissions have been the focus of particulate matter reduction efforts, but as these emissions are decreasing due to these efforts and the improvement of diesel engines, the focus is expected to shift to non-exhaust particulate matter emissions, which is projected to drastically overtake exhaust PM in the coming years.

Today, braking in internal combustion engine (ICE) vehicles is done using the friction between two materials to decelerate or come to a stop, and with this reaction between the two friction materials come heat and debris from the materials, some of which is airborne in the form of particulate matter. However, electric vehicles (EV) and hybrid vehicles employ both friction braking and regenerative braking, which is another factor that must be taken into consideration when looking at the future of braking emissions, as EV sales are projected to increase by 24% annually until 2030 [8]. Braking emissions are dangerous considering the metals used in braking friction materials such as iron, copper, titanium, and zinc, and therefore it is important to understand how to decrease these emissions by changing friction material properties and switching to the use of electric vehicles.

As aforementioned, this thesis studies the future of braking systems with respect to particulate matter emissions. A test procedure for measuring braking particle emissions has been developed at Volvo Cars Corporation, and three brake pad materials and two braking cycles (one for internal combustion engine vehicles and one for electric vehicles) have been studied and compared against each other with respect to braking particle emissions. Before and after the tests, material analysis of the friction surfaces was done to understand how the different materials react with one another and how this affects the particulate matter emissions in order to better understand what friction materials can be recommended for future braking systems. The particles were also captured and studied to estimate their potential threat to human health.

The three brake pad materials that have been chosen in the scope of this thesis are semi-metallic (European market), non-asbestos organic (United States and Asian markets), and a new, altered non-asbestos organic brake pad designed with the aim to reduce particulate matter emissions. These materials were chosen to determine the best option for brake pads on the market now with respect to brake emissions and the braking cycles used were chosen to represent typical, every day driving in ICE vehicles and EVs. However, the test setup has been designed such that it can be repeated again at Volvo Cars Corporation to test other brake pad and disc materials as they are developed and improved for emissions reduction. This thesis determines how braking particulate matter emissions can be reduced by changing friction material or switching from an ICE vehicle to an EV, and suggests brake pad material for the future in order to minimize environmental impact.



5 Braking Systems

In this section, an overview of traditional braking systems will be given. These systems include friction braking, and now with the increasing electrification of the vehicle market, regenerative braking as well. The braking system of a vehicle is responsible for allowing the vehicle to slow down, or bringing the vehicle to a stop. The fundamental concept of braking is related directly to the law of the conservation of energy: energy cannot be created or destroyed. Energy is needed to accelerate a vehicle, and therefore energy must be removed or transferred to decelerate a vehicle. In the case of friction braking, this energy is dissipated in the form of heat, and in the case of regenerative braking, this energy is stored and reused again when the vehicle is accelerated.

The equation for the kinetic energy involved with decelerating a vehicle, E_{decel} from velocity v_2 to velocity v_1 is as follows:

$$E_{decel} = \frac{1}{2}m(v_2^2 - v_1^2) \quad (5.1)$$

Where m is the mass of the vehicle in kilograms. The value calculated of E_{decel} is essentially the amount of energy that needs to be absorbed thermally in a friction brake (or stored in the case of regenerative braking).

5.1 Friction Braking

5.1.1 Friction Braking System Overview

Friction brakes in the automotive industry predominantly consist of disc brakes, however drum brakes are still used on the rear axle of some vehicles. Drum brakes were replaced with disc brakes because of their problematic thermal fade. The key components of a disc brake system are shown in Figure 5.1 and will be described individually.

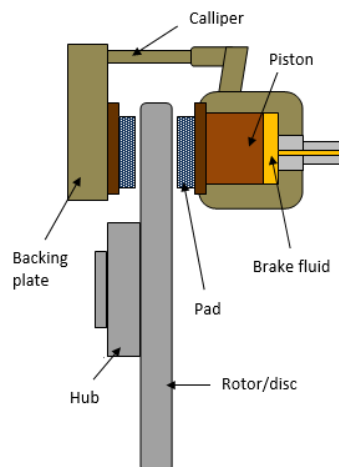


Figure 5.1: Side Profile of Disc Brake [1]

- **Rotor/Disc and Hub:** These components of the braking system are fixed to the wheel bearing and axle of the car. Therefore applying a frictional force to the surface of the disc will slow it down and therefore slow the vehicle down. The brake disc is designed and materials selected such that it can easily dissipate the heat created by contact with the brake pads in order to stop or slow the vehicle. It is most commonly composed of gray cast iron, but some other materials include aluminum, ceramic, or even stainless steel depending on the application. This will be discussed further in section 8.2.
- **Brake Pad:** The brake pads are the components made up of friction materials (these materials are discussed in section 8.1) that come into direct contact with the brake disc to create friction and heat, and ultimately slow or stop the vehicle.
- **Backing Plate:** This is a thin (usually metal) lining bonded to the friction material of the brake pad that serves to help evenly distribute the braking pressure across the brake pad.
- **Piston/Brake Fluid:** The force pressing the brake pads to the disc is controlled by the brake fluid and piston. The compression of the brake pedal in the vehicle dictates the brake fluid flow and pressure in the piston, and therefore controls the amount of braking force applied.
- **Caliper:** The caliper is the component of the braking system that serves as a housing to hold the brake pads and piston(s) in place and allows their movement. In general there are two types of calipers: sliding calipers and fixed calipers. Figure 5.1 shows a sliding caliper, which means there are only one or two pistons applied to the brake pad on one side of the disc, and the caliper can slide such that the brake pads on both sides of the disc have contact with the surface. Fixed calipers consist of a non-moving caliper and one or two pistons behind both brake pads. Guide pins are used in a sliding caliper to let the housing move freely, whereas the guide pins of a fixed caliper serve to control only the motion of the brake pads. The sliding caliper is the most common type of caliper.

5.1.2 Friction Braking Performance Parameters

The friction braking system is one of the most important components of a vehicle with respect to safety. For that reason, friction braking systems usually undergo extreme braking performance tests, such as the AMS test developed by Auto Motor und Sport magazine. This test includes 10 full stops consecutively from 130 km/h to 0 km/h at a level of deceleration of 0.8g's (7.85 m/s^2) [9]. Some of the parameters crucial for brake performance that are focused on in this thesis are described below:

- **Magnitude of Deceleration:** The capability of a friction braking system is obviously dependent on the braking force or slow-down required.
- **Disc Temperature:** The temperature of the brake disc affects the performance and effectiveness of the braking system. As said before, friction between the pad and disc is used to convert the kinetic energy of the vehicle into thermal energy. Therefore, the disc and pad are absorbing heat during braking.
- **Coefficient of Friction:** The coefficient of friction is used to quantify the amount of friction between two surfaces. It is a unitless value denoted as μ and has a minimum value of 0 referring to no friction between the surfaces. A typical coefficient of friction value for friction materials is 0.4. The coefficient of friction between two materials is highly nonlinear with respect to temperature, but the value decreases when temperature is significantly higher than normal operating temperatures.



5.2 Regenerative Braking

The concept of regenerative braking essentially encompasses any braking system where the kinetic energy of the vehicle is stored during deceleration to be used during acceleration. This implies that there must be a form of energy storage in the vehicle to hold this energy until it is needed for acceleration, which can be done with a battery in the most common case of a hybrid or electric vehicle, or for example in compressed air/fluid with a hydraulic power assist (HPA) system, or a flywheel.

However, in this thesis, the main focus will be regenerative braking systems used for hybrids and electric vehicles, reflecting the market trend towards electrification. To go into more detail about this system and how it works, please refer to Figure 5.2 [2].

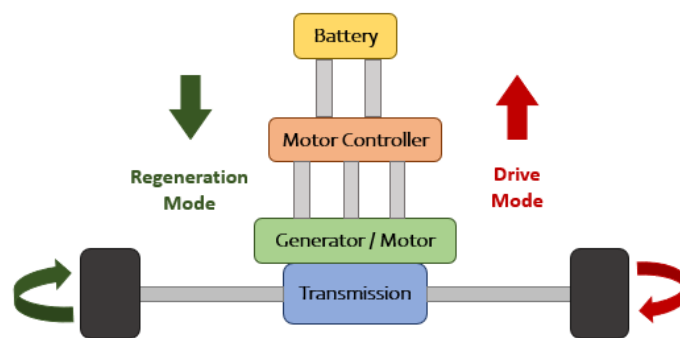


Figure 5.2: Regenerative Braking Map in an Electric Vehicle [2]

In drive mode, or acceleration mode, the energy stored in the battery is used to power the motor and translate electrical energy into rotational mechanical energy that propels the car forward. In regeneration mode, or deceleration mode, the rotational mechanical energy of the wheels turning is coupled to the motor which begins to act as a generator, producing electrical energy from mechanical energy and simultaneously slowing the vehicle while transferring the electrical energy produced by the generator into the battery to charge it.

The important implication with regenerative braking systems is that these systems are able to almost completely slow the vehicle with little or no help from the friction braking system, depending on the application. As more vehicles become electrified on the road, this will have large implications for the size and design of the friction braking system in the future.

6 What Are Braking Emissions?

Braking emissions are the airborne particles that become removed from friction surfaces of the brake system as a result of braking events. These brake wear particles can be very difficult to quantify in the field, since there are so many other sources of particulate matter present with regards to vehicle transportation including exhaust emissions, road wear/dust, tire wear, and re-suspended particles from the road. However, braking emissions are increasingly becoming a subject of concern due to their metal content, and as heavy regulations on exhaust emissions have been executed, non-exhaust emissions are expected to be the next object of focus.

Particulate matter is in general classified by its aerodynamic diameter. The most common classifications are PM10 and PM2.5, however PM1 is also becoming a prominent category. PM10 accounts for the measurement of all particles with an aerodynamic diameter of less than $10\mu m$, PM2.5 less than $2.5\mu m$ and PM1 less than $1\mu m$. Particle measurements are traditionally assessed in mass $\frac{\mu g}{m^3}$, or in count $\frac{\text{number of particles}}{m^3}$. The quantity and size of braking emission particles depend on several factors, the most notable being the friction materials used for disc and pad, which will be the focus of this research. The size and type of the braking system (i.e. drum versus disc) also play a role in addition to the vehicle parameters such as initial speed, brake temperature, and magnitude of deceleration.

6.1 Environmental and Health Concerns

Exposure to air pollution, particularly in the form of particulate matter, has been associated with acute and chronic effects on health in humans. According to the Environmental Protection Agency (EPA) of the USA, scientific studies have linked particulate matter exposure with nonfatal heart attacks, premature death in people with lung or heart disease, irregular heartbeat, aggravated asthma, decreased lung function, and increased respiratory issues. Furthermore, the International Agency for Research on Cancer has attested that ambient air pollution, and especially particulate matter, is carcinogenic to humans [10].

Of the different sources of particulate matter, transport-related particulate matter is of particular concern because of their composition, and because they are mostly smaller, fine particles, which are more at risk of entering the respiratory tract and circulatory system. That being said, there lacks sufficient studies regarding the health effects directly caused by non-exhaust particulate matter emissions, not to mention specifically brake wear emissions. This is despite the fact that some estimates of non-exhaust particulate matter emission contributions to total traffic particulate matter emissions are approximately 50% [6]. It is very difficult to quantify the fractions of exhaust and non-exhaust particulate matter because it is hard to distinguish between them, and tests for exhaust emissions are very developed, while studies for non-exhaust emissions, and particularly braking emissions, are relatively premature and undeveloped [6].

However, some key harmful particles, mostly with metal composition, have been identified as traces of non-exhaust particles and associated with adverse health affects: Fe, Al, Cu, Zn, Ca, Ni, V, Ti, Cr, Mg, S, Si, K, and Mn. The most prominent evidence that links brake wear to adverse health effects is oxidative stress occurring in the cells, since this is caused pointedly by metallic particulate matter, which is known to be the composition of much of the particulate matter coming from brake wear emissions. Oxidative stress is a term used to describe the imbalance between antioxidant and pro oxidant agents in the body. Particulate matter particles from brake wear contain organic compounds and metals, which serve as pro oxidants, having a single unpaired electron, therefore making them highly reactive and able to start a chain reaction in the body, causing cellular damage [6].



Studies have been conducted to show the long term effects, or chronic effects, as well as the short term, or acute effects, of particulate matter exposure. Short term can be described as daily or hourly exposure to PM emissions causing an acute response, while long term can be described as annual exposure causing chronic health deterioration [6]. Fulvio Amato's book "Non-Exhaust Emissions" [6] gives an overview of these two categories of health effects.

In the tables below, different studies conducted to analyze the short and long term effects of exposure to traffic related non-exhaust PM have been summarized, detailing the health effects observed, as well as the specific elements found that related the PM to non-exhaust sources. These tables summarize only some of the studies done—shown are the studies that found the most prominent elements and serious effects, though there are more mentioned in [6]. (**Note:** CVD, cardiovascular; RESP, respiratory; MI, myocardial infarction; CHF, congestive heart failure; DIAB, diabetes; CRP, c-reactive protein.)

Author, Date. Journal	Health Effects	PM size	Cu	Al	Zn	Ni	Fe	Cr	V	S
Samoli, 2016. Occup Environ Med	CVD and RESP hospitalizations	PM10 PM2.5	x	x	x					
Basagana, 2015. Env Int	cause-specific mortality and admissions	PM10 PM2.5	x		x	x	x		x	
Valdes, 2012. Environ Health	cause-specific mortality	PM2.5	x		x			x		
Bell, 2012. Res Rep Health Eff Inst	morbidity	PM2.5				x			x	
Bell, 2009. Respir Crit Care Med	CVD and RESP admissions	PM2.5				x			x	
Zanobetti, 2009. Environ Health	admissions for CVD, MI, CHF, RESP, DIAB	PM2.5				x		x		
Franklin, 2008. Epidemiology	all-cause mortality	PM2.5		x		x				x
Ostro, 2007. Environ Health Perspect	all-cause mortality, CVD, RESP	PM2.5	x		x					
Lippmann, 2006. Environ Health Perspect	all-cause mortality	PM2.5				x			x	

Table 6.1: Short Term Effects from Components of Non-Exhaust PM Emissions

Author, Date. Journal	Health Effects	PM size	Cu	Al	Zn	Ni	Fe	Cr	V	S
Wang, 2017. Epidemiology	mortality	PM2.5	x				x			
Raaschou-Nielsen, 2016. Env Int	lung cancer	PM10 PM2.5	x		x	x				x
Wolf, 2015. Epidemiology	incidence coronary events	PM10 PM2.5					x			
Hampel, 2015. Env Int	biomarkers CRP fibrinogen	PM10 PM2.5	x		x		x			
Beelen, 2015. Environ Health Perspect	natural mortality	PM10 PM2.5								x
Eeftens, 2014. Epidemiology	lung function in children	PM10 PM2.5				x				x
Fuertes, 2014. Int J Hyg Environ Health	early life pneumonia	PM10			x					
Basu, 2014. Environ Res	birth weight	PM2.5	x		x		x		x	x
Ostro, Environ Health Prospect	natural and cause-specific mortality	PM2.5			x		x			

Table 6.2: Long Term Effects from Components of Non-Exhaust PM Emissions

6.2 Proposed Legislation for Non-Exhaust PM Emissions

Currently, there does not exist an enforced regulation on non-exhaust PM emissions. However, as exhaust PM emissions have been on the decline for the past decade or so, the focus is shifting more towards the regulation of non-exhaust PM emissions since they are comparatively becoming more prominent. Furthermore, metals are some of the most problematic particles, and these are heavily regulated in exhaust and the industry in general. Therefore it can be predicted that non-exhaust emissions are becoming the largest contributor to metal particles in urban air [6].

There did exist, however, some projects funded by the European Union to analyze the harmful effects of braking emissions. One is an initiative project called REBRAKE coordinated by Freni Brembo Spa, Kungliga Tekniska Högskolan, and Universita Delgi Studi Di Trento that took place from 2013-2017. The main objective of this project was to decrease braking PM10 emissions by 50% mass in order to prepare for the EU2020 goal of a 47% decrease in particulate matter. This was done by gaining a better understanding of the materials and interactions between friction materials in braking systems, resulting in a new brake pad and disc design and composition. The composition proposition also took into consideration the trend of eliminating copper in brake materials, which is discussed more below [11]. Another EU-funded project regarding brake system sustainability is LOWBRASYS, also coordinated by Freni Brembo Spa, which took place more recently from 2015-2019. The goal was to develop a "low environmental impact braking system" by decreasing the PM braking emissions by 50%. In order to achieve this goal, the project worked with the braking system materials and control systems for braking [12].

The regulations that apply to the production of braking materials are mostly general material bans or regulations. For example, asbestos was a popular friction material that is now totally banned in most of Europe and many countries around the world, or at least regulated in others. Furthermore, in the USA state of California, it

was estimated that 35-60% of copper in runoff water was from braking materials. This led to a regulation in Washington and California states aimed at phasing-out of copper in brakes, with the end goal of less than 0.5% copper by weight in brakes by January 2025 [6].

The Registration, Evaluation, Authorization, and Restriction of Chemicals (REACH) is a Europe-adopted regulation with the goal of "better and earlier identification of the intrinsic properties of chemical substances," in order to protect the environment and human health. Essentially materials must be registered for a specific application, otherwise they cannot be used. This is attempting to avoid the potential risk of widely adopting the use of a new material without knowing the full extent of health and environmental hazards associated with it. There are also REACH-like initiatives in many countries outside of Europe such as China and the USA [6].

6.3 Capturing and Measuring Braking Emissions

Three case studies were analyzed in the scope of this work. The reason for this analysis was to understand state of the art practice to measure braking emissions. The first braking emissions test data reported is a study overseen by the Environmental Protection Agency of the USA [10]. This study, done in 1983, was for asbestos brake pads which are now banned. Listed below are a few more recent studies that have been cited numerous times in literature regarding braking emissions. Researching previous braking emission studies helped to shape and develop the test procedure used for this thesis.

6.3.1 Case Studies

General Motors, 2000

The first published braking emission study done using an inertia dynamometer test was conducted at General Motors (GM) in 2000, analyzing the particulate matter emissions of seven types of brake pads that represented the brakes of 88% of GM's production two years prior. Seven different brake pad materials were tested, of which six were pads for disc brakes and one was a shoe for a drum brake. These tests were done for four different brake surface temperatures: 100°C, 200°C, 300°C, and 400°C, which were measured via a thermocouple in the rotor, and were achieved by altering the speed of the airflow around the brake system and the frequency of the braking events [13]. The braking events used were a constant deceleration from 50 kmph to 0 kmph at a deceleration rate of 0.3g.

Particle mass distributions were determined using a micro orifice uniform deposit impactor (MOUDI), while particle number distributions were determined using a Dekati electrical low-pressure impactor (ELPI). The MOUDI measures particle size by forcing the particle-ridden air onto a series of impaction plates (in this case five were used, ranging from 18 to 0.1 μm) that collect smaller particles as they proceed, so the size distribution of the particles can be determined in terms of their aerodynamic diameter quite nicely. The ELPI is a thirteen stage impactor measuring real time particle size distribution. Additionally, an electrical aerosol analyzer (EAA) was used continuously to count the number of particles and measure their aerodynamic diameters if larger than 0.01 μm , since the ELPI does not have the capability to measure particles that small.

The biggest finding from this study characterized the relationship between disc temperature and particle emissions, showing that as the disc temperature rises, the particle emissions increase drastically [13].



Ford Motors Research Laboratory, 2003

In these tests, three different types of brake pad materials were tested with respect to particle emissions: low metallic, semi-metallic, and non-asbestos organic, representing 90% of brake pads being used in the automotive industry at the time [14]. The pads were worn for approximately 1000 stops before measuring the emissions to ensure stable wear. Two driving cycles were used: one "Urban Driving Program" consisting of 24 mild and low speed stops, and one braking test cycle from "Auto Motor und Sport Magazine" consisting of 10 stops from 100 kmph to 0 kmph.

MOUDI and ELPI devices were also used in this application to measure the size distribution of the particles. The aluminum foil collection substrate from the MOUDI device was weighed after to determine the mass-weight distribution. The results show that about 50% of the brake wear emissions were airborne, and the average particle size by mass was $6\mu\text{m}$ while the average size by number count was $1-2\mu\text{m}$ [14]. Elemental analysis was done on all particle emissions - both airborne and deposited particles found on the braking system.

Japan Automobile Research Institute, 2015

Other brake wear emissions tests were conducted on a dynamometer in Japan's Automobile Research Institute. The braking assemblies chosen for testing were ones that covered 73% of the Japanese passenger car market and 30% of the Japanese truck market between 2005 and 2010. For these tests the brake system was in a closed chamber (110 x 30 x 60 cm) with a constant speed airflow to simulate real-life driving conditions. The Japanese transient emissions test cycles, which represent driving on an urban road with maximum speed of around 85 kmph, were used to test the braking systems, and three types of emissions were measured: the fallout emissions onto the road (particles that were emitted and fell to the tray for collection at bottom of the test chamber), deposition on the brake pad and disc surfaces, and lastly, the airborne particles. The particles deposited onto the braking system surfaces were removed with a micro spatula and brush, while the airborne particles were collected using four multi-cascade impactors- two for $\text{PM}_{2.5}$ and two for PM_{10} , three 12-stage impactors, and an HV- $\text{PM}_{2.5}$ for isotope analysis [15].

This study only took into account the emissions of the brake pads, which was done by disregarding any particles with iron (Fe), as these were most likely to come from the brake disc [16]. Of the three vehicles tested, two vehicles had disc brakes and showed similar mass fractions of PM_{10} and $\text{PM}_{2.5}$, whereas the third vehicle was a drum brake and showed almost the same mass fraction of PM_{10} and $\text{PM}_{2.5}$, meaning there were few particles between the aerodynamic diameter of $2.5\mu\text{m}$ and $10\mu\text{m}$. However, all vehicles demonstrated that the highest amount of emissions being produced at the highest level of deceleration and highest speed [15].

6.3.2 Summary: Moving Forward

To summarize, most of the analyzed case studies in the previous section have used various forms of impactors to measure particle size distribution, and a brake dynamometer (either closed or open chamber) to simulate the braking events. The specifics on the test setup and data collection proposed for this thesis will be discussed in depth in further section 10.1.



7 Electrification in the Automotive Industry and Impact on Braking Emissions

7.1 The Future of Braking Systems and Braking Emissions

As mentioned in the previous chapter, non-exhaust emissions are projected to make up a majority of transport-related PM emissions in the coming years. This is due to regulations on exhaust and combustion emissions, but also due to the transition to hybrids and electric vehicles which produce zero exhaust emissions on the road. With the trend of increase in electric vehicle sales by at least 24% annually until 2030, by then they are expected to be 6% of the light duty vehicle fleet [8]. Therefore, non-exhaust braking emissions are also expected to decrease as electric vehicles rely more heavily on regenerative braking, as discussed more in the next section.

Another future trend for vehicles that should be considered with respect to braking emissions is autonomous driving vehicles, which are now being actualized. Autonomous vehicles are vehicles that are able to operate themselves fully or partially without a human operator. Autonomous vehicles are able to detect their environment with sensors in order to make decisions about acceleration and deceleration. In the case of deceleration, a technology called Predictive Efficiency Assistant (PEA) uses a GPS to determine the need for deceleration based on speed limit and topography, therefore doing it most efficiently and comfortably for the passengers [3]. Furthermore, the ability for the car to drive itself during cruising will remove the human error from the driving experience, not only making traveling by car safer, but consequently reducing the need for braking since deceleration will be anticipated by the sensors, PEA, or GPS of the vehicle rather than the driver.

In the future it can be expected that there will be less need for the friction brake because of increased regenerative braking for efficiency in hybrids and electric vehicles, and also because of less aggressive braking patterns experienced in autonomous driving vehicles.

7.2 Future EV Impact on Braking Emissions

This section will discuss how the projection for electrification of the automotive industry will have an effect on PM emissions from braking due to the decreased use of the friction brakes, and increased use of regenerative braking. In an electric vehicle, the amount of braking energy that can be taken care of by regenerative braking is dependent on several factors, including: battery state of charge, ambient/battery temperature, and motor performance. But in general, to increase the efficiency of the vehicle, regenerative braking should be maximized as much as possible since friction braking is transferring kinetic energy into waste heat energy from which nothing is gained. Figure 7.1 shows the distribution between the friction brakes and regenerative braking in a typical electric vehicle [3].

The three different sections of the braking event portrayed in Figure 7.1 are described as follows:

1. **Brake Initiation** This is the beginning of the braking event when the pedal is actuated by the driver, giving a deceleration demand to the control unit of the vehicle. The friction brake is activated immediately to cover most of the original braking demand until the motor can supplement. This is done because of something called "the pedal feel". The driver should experience a linear pedal feel for maximum comfort, meaning that when the brake pedal is compressed, the deceleration of the vehicle should be correlated



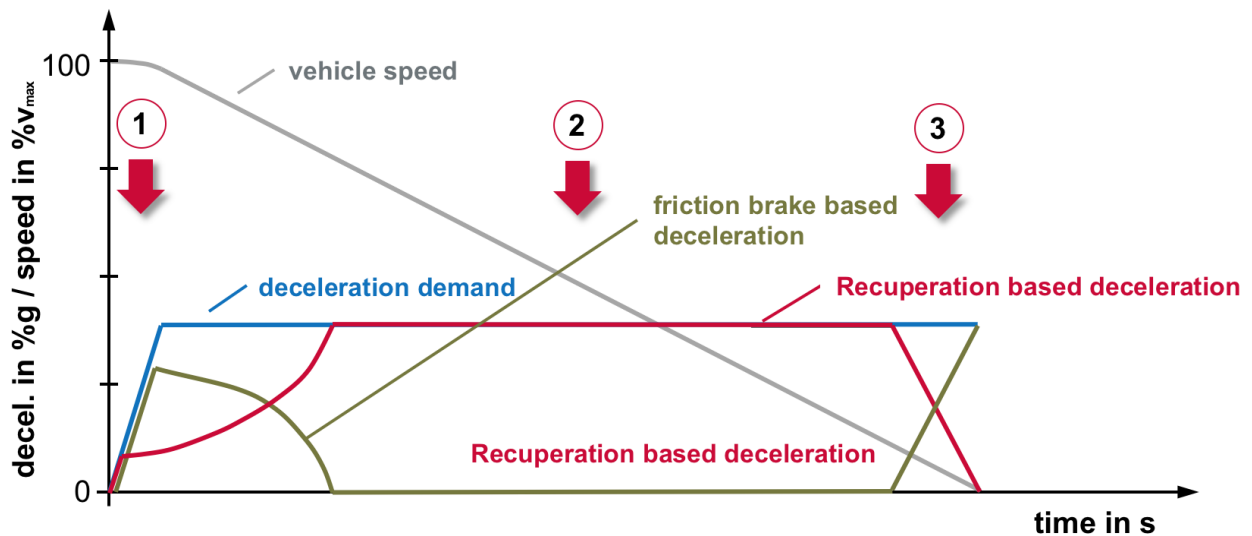


Figure 7.1: Brake Blending Between Friction Braking and Regenerative Braking [3]

linearly to the amount that the pedal is compressed. The driver also wants to feel deceleration immediately upon actuation of the brake, which makes it important for the friction brake to be used.

2. **Full Recuperation** This is the period in which the braking demand is constant and the electric motor is able to cover 100% of the braking demand, so the friction brake is not necessary [3].
3. **Near Standstill** This period is when the vehicle is reaching low speeds and it becomes inefficient to use the electric motor for braking. Therefore the friction brake takes over the braking demand until the vehicle reaches a stop [3].

Ultimately, the friction brake is used in an electric vehicle to enhance the brake pedal feel in the beginning of a braking event, when the motor is not efficient for energy conversion at low speeds toward the end of a braking event, to stand still, and also during emergency heavy braking cases. As can be seen in Figure 7.2, much less friction braking pressure is used in an electric vehicle [3]. Therefore, it is predicted that an electric vehicle will help to reduce particulate matter emissions by decreasing the use of the friction brake drastically.

The reduced use of the friction brake and lower braking pressures in general also result in a decrease in the operating temperature of the brake disc. Some studies, such as that shown in Figure ?? [13], show a strong correlation between drastic increase of particle emissions and higher brake disc temperatures. However, as can be seen in Figure 7.2, the normal operating temperature of the disc is much lower in that of an EV, which should also help to mitigate brake particle emissions.

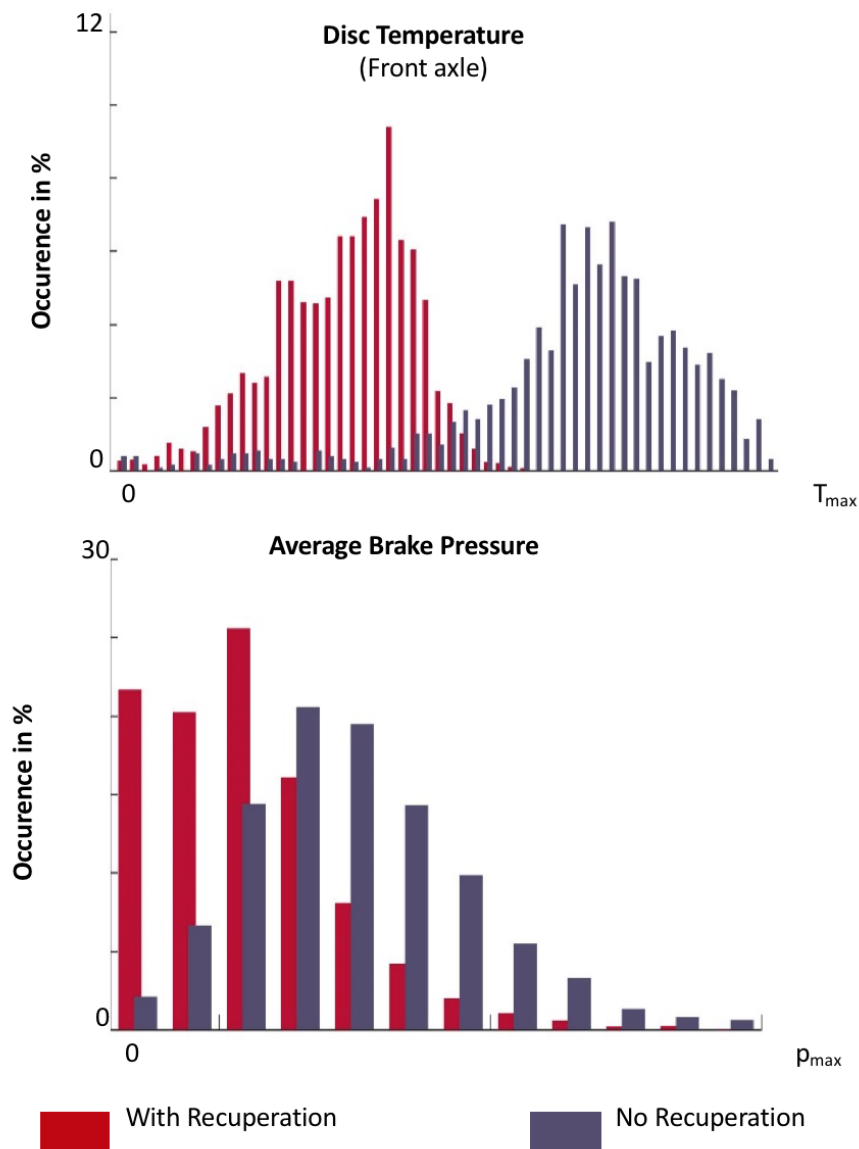


Figure 7.2: Disc Temperature and Brake Pressure for ICE vs. EV [3]

7.3 Projection for Braking Emissions

Using the results found in this thesis quantifying the difference in brake particle emissions for ICE vehicles and EVs and making some assumptions, it can be predicted how the electrification of the automotive industry and decreased use of the friction brake will affect the level of PM emissions in the coming years. In order to make an estimation of this projection, three values must be assumed in addition to the data found in this study: the contribution of brake particle emissions annually, the trend of increase for brake particle emissions in the future, and the trend of increase in percentage of electric vehicles on the road in the future.

Brake Particle Emissions Annually

First, the emissions scenario for PM from brakes needs to be estimated currently. As mentioned previously, brake wear and non-exhaust emissions in general are a premature study subject and difficult to distinguish from one another, and therefore it is difficult to find data about how much of each emission source is contributing. However, the National Atmospheric Emissions Inventory of the United Kingdom (UK) gives concise data regarding the different non-exhaust emissions sources: brake wear, tire wear, and road dust suspension, in comparison with the exhaust emissions of PM_{2.5}. Therefore this data will be used for the estimation.

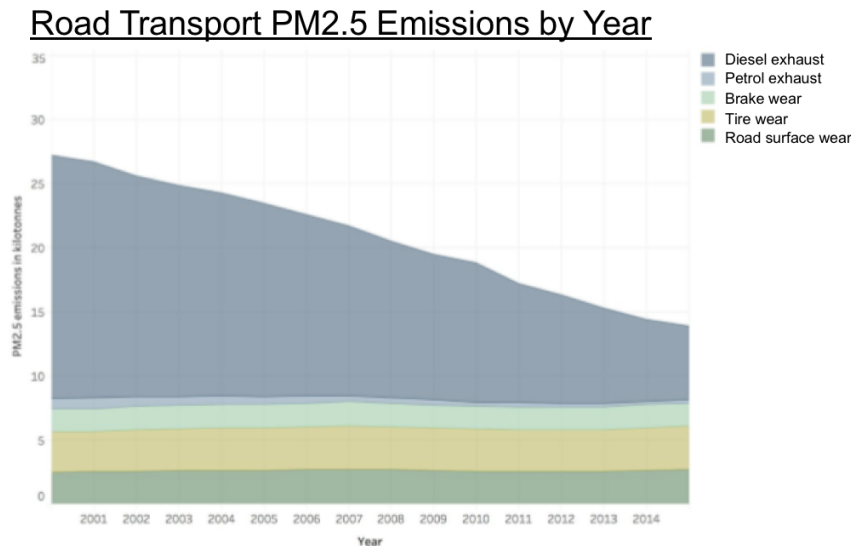


Figure 7.3: Road Transport PM_{2.5} Emissions Sources by Year in United Kingdom [4]

As can be seen in Figure 7.3, exhaust emissions have drastically decreased from 2000-2015, comparatively putting non-exhaust emissions in the spotlight, as they have increased slightly during the same time period. According to this data, brake wear in 2015 was contributing approximately 1.6 kilotonnes of PM_{2.5} emissions, in other words making up about 20% of the non-exhaust emissions.

Trend of Increase in Brake Particle Emissions

The trends for the coming years with respect to non-exhaust emissions were predicted to see how braking emissions will change in time. As can be seen in Figure 7.4, it is projected that non-exhaust emissions will increase in time. However, since prior to this thesis, there have not been any published studies conducted to quantify the affects of regenerative braking on braking emissions, this trend projected also by the UK does not take into account electric vehicles [4]. This study predicts that non-exhaust emissions will increase in contribution to PM_{2.5} from 8 kilotonnes to roughly 9.5 kilotonnes by 2030.

If it is assumed that brake wear, tyre wear, and road surface wear increase equally in the coming years, then it can be estimated that braking particle emissions will increase from 1.6 kilotonnes contribution to 1.9 kilotonnes by 2030 according to this study.

Projected PM2.5 Emissions from Road Transport

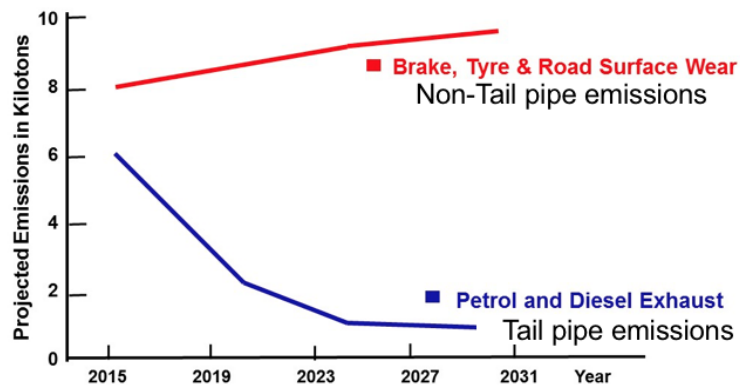


Figure 7.4: Predicted PM2.5 Levels due to Exhaust vs. Non-Exhaust Sources until 2030 in United Kingdom [4]

Trend of Increase in Electric Vehicles

There are many different predictions as to how many electric vehicles will be on the road by 2030. For example, the Global EV Outlook [8] predicts the amount of EVs on the road until 2030. This study conducted by the International Energy Agency predicts two scenarios:

1. **New Policies Scenario** This scenario only accounts for sustainability policies that exist or have been announced in order to predict the number of EVs on the road by 2030. With this projection, it is predicted that the electric vehicle fleet will reach about 130 million by 2030.
2. **EV30@30 Scenario** This scenario reflects changes made if aggressive policies are made in the future to meet climate goals. Its name refers to the EV30@30 Campaign Declaration in which EVs hold a 30% market share globally by 2030. With this scenario's prediction, the electric vehicle fleet will reach 228 million by 2030.

Though the total number of EVs is predicted for 2030 for both of these scenarios, the total estimation of the vehicle fleet for 2030 is not given in this report, and therefore makes it difficult to foresee the effect on braking emissions.

Another study done by Bloomberg New Energy Finance [5] predicts the global trend for electrification of the vehicle fleet as seen in Figure 7.5, with less than 1% in 2015 increasing to 7% in 2030. Though this estimation is only for light-duty vehicles, these values will be used for the prediction since light-duty vehicles will make up 95% of the vehicle fleet by 2030 [17].

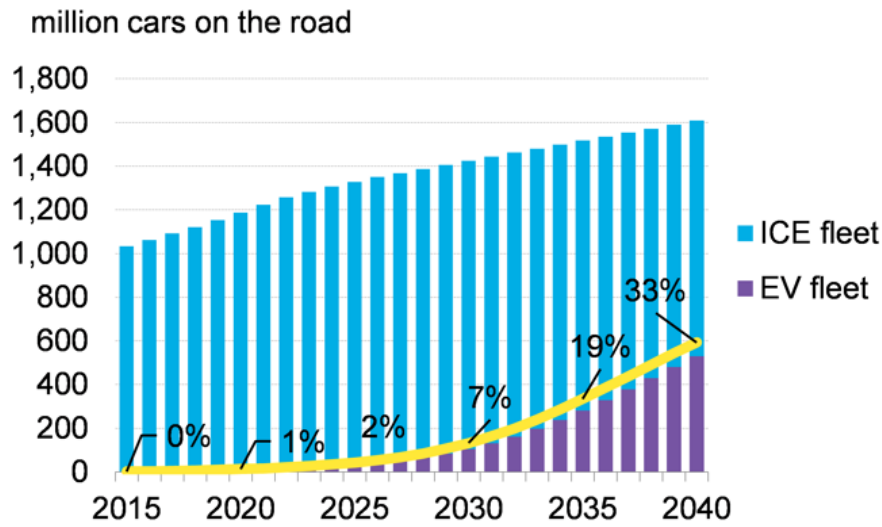


Figure 7.5: Global Increase in Electric Vehicle Fleet vs. ICE Fleet [5]

Putting the Numbers Together

Now that all of the numbers have been gathered to make an estimation, the calculation can be made. From the results in this thesis, it is assumed that an EV emits 49.6% of the PM2.5 emissions as compared to that of an ICE vehicle. Given the conservative projection of an EV fleet making up 7% of the total vehicle fleet in 2030, it can be predicted that the total PM2.5 contribution from braking emissions will decrease from 1.9 kilotonnes to 1.83 kilotonnes in the case of the United Kingdom, or in other terms, roughly a 4% decrease in braking PM2.5 emissions by 2030.

While this amount may seem small, the conservative assumptions used in this calculation suggest that this could be a very minimum change in braking emissions in the future. As can be seen with the Global EV Outlook conducted by the International Energy Agency, there are many different scenarios that could affect the contribution of EVs to the vehicle fleet in the future. Furthermore, the braking cycle used in this thesis is still assuming that the friction brake is used to provide 30% of braking force in EVs, but future trends lean towards the use of the motor for 100% of braking force in order to maximize efficiency of electric vehicles.

8 Brake Disc and Brake Pad Materials

The whole purpose of friction brakes is to decelerate by transforming the kinetic energy of the vehicle into heat by friction and dissipating that to the surroundings. Thus, the materials used in these applications are expected to perform at higher levels of temperature and be more durable. Important material requirements for automotive brake applications are thermal diffusivity, resistance to corrosion, weight, good noise vibration and hardness (NVH) performance, stable coefficient of friction, and low wear rate coupled with acceptable cost and working life [18].

Historically, there has been a tremendous evolution in brake materials. Wagon brakes started using wood and leather at first and then gradually experiments were conducted in 1800's with iron brake shoes to meet high load and speed requirements demanded by railroad technology. Herbert Froad first invented the brake lining material in 1897 [18]. It was a cotton based material impregnated with bitumen solution and was used in early automobiles. Technology has evolved since then, increasing the demands placed on the friction material. In order to achieve the current requirements, most friction materials today are composed of a combination of several materials. More than 2000 material variants are used today in commercial brake components [18]. Detailed discussion on the brake pad and brake disc materials is done in subsequent sections

8.1 Brake Pad Materials (Friction Materials)

A brake pad material or friction material has a complex material composition as it is expected to match the higher demands in brake performance. These materials serve a variety of functions which are responsible for efficient braking. A typical brake brake pad in an automotive application consists of 12 to 14 ingredients which are blended and processed based on their characteristics to produce a complex friction material [18]. So, it is a heterogeneous material with a combination of different additives like abrasives, friction modifiers, fibers/reinforcements, and binder materials. Although this is a general categorization, some of these additives can be placed into several categories. These material constituents are held together by a polymeric binder which is normally a thermosetting polymer. Braking phenomenon results in the wear of both disc and pad material which is essential.

Although the manufacturing process of a brake pad depends on the type of ingredients used, the general steps are:

1. Shot blasting of the base plate
2. Ultrasonic cleaning
3. Glue application
4. Hot press moulding
5. Heat treatment
6. Surface Spraying
7. Slotting and Chamfering

Wear in the pad material occurs differently, ranging from light abrasion of hard phases to adhesive pullout. The wear process will be discussed in detail in section 9. Ingredients used, coupled with manufacturing process followed determines the final brake pad quality. Variation in additive composition by a small percentage can affect the brake performance. Apart from the additive composition, features like porosity, density, moisture etc. affect the surface properties and thereby the brake performance. Some amount of porosity (5-30 percent) is usually present. The variation in porosity level can affect the brake performance [19]. The lower the porosity



level, the higher the adhesive propensity between brake pads and disc due to increased contact area between them. Rockwell hardness decreases with increasing porosity percentage especially between 13-22% [19] possibly due to lower densities. Below, the major additives present in a brake pad are briefly discussed. This is just a general classification but it can be non-exhaustive.

The overall mechanical properties of friction materials largely depends on the interfacial characteristics which are quite complex. The efficiency of chemical and mechanical bonding between different additives determines the interfacial strength. This in turn affects important parameters like elastic modulus, tensile strength, density, coefficient of thermal expansion etc [20]. Even though these parameters can be estimated from the fibre arrangement, fibre properties, volume fractions of the matrix and fibres, the rule of mixtures cannot be applied here as the properties depend on the spatial arrangements and disposition. This is further explained in 8.1.3. Thermal fatigue failure in brake pads is expected and to avoid this, the thermal expansion coefficients of the matrix and fibres must be minimized. This can be achieved by having oxide layers in between which act as fibre coating easing the thermal stresses at interfaces [20].

8.1.1 Abrasives

Abrasives are required to control the build-up of friction films which results in increased friction, particularly when the vehicle is decelerating. The importance of friction layer is explained in 9 and it is believed that wear rate decreases due to the friction layer build up [20]. The table below shows examples of abrasives used in a brake pad [18].

Material	Description / Remarks
Aluminum Oxide	Hydrated form added as a polishing agent for wear resistance. Anhydrous form is more abrasive, whereas fused form is the hardest and most abrasive form.
Iron oxides	Fe_2O_3 and Fe_3O_4 are mild abrasives
Quartz	Crushed mineral particles (SiO_2)
Silica and Zirconium silicate	May be naturally or synthetically produced

Table 8.1: Abrasives used in brake pads

8.1.2 Friction Modifiers

Friction modifiers are usually solid state lubricants which raise the friction or create inter facial films by forming oxides. These compounds have have lower melting point when compared to abrasives. Lead and lead oxide used earlier, were the most wildly used friction modifiers. But today they are banned due to toxicity. The table below lists some example friction modifiers [18].

Material	Description / Remarks
Graphite	Low cost and most used. Burns in air at >700deg C. Friction can be affected by moisture
Ceramics	Alumina-Silica mix with minor Iron or Titanium oxides. Low density filler which reduces rotor wear and controls friction. Also, absorbs rotor dust
Copper	Causes excessive cast iron wear
Friction dust and Friction powder	Mostly consists of cashew resin and some rubber base. May consist of Fe Sponge in some cases. Used to reduce spontaneous combustion or help particle dispersion
Lead oxide	Has Toxicity concerns
Metals	Pb, Sb, Bi, Mo serve as oxidizers to stabilize friction-induced films. Responsible for constant wear rate.
Metal oxides	Fe ₃ O ₄ improves cold friction, ZnO lubricates and CrO ₃ raises friction
Metal sulphides	Cu ₂ S, Sb ₂ S ₃ , PbS modify and stabilize coefficient of friction. PbS- reduce wear and noise. MoS ₂ facilitates adhesive friction. ZnS a low cost solid lubricant for high loads and temperatures.
Mineral fillers	Mullite, Kyanite, Silimanite, Alumina are fragile and control wear on the counterface

Table 8.2: Types of Friction Modifiers

8.1.3 Reinforcements/Fibers

Reinforcements or fibers play a critical role in absorbing stresses by wet engagement process. They maintain the integrity of the composite at elevated temperatures [21]. Fibers provide increased mechanical strength to the friction material by absorbing the shear loads over the entire braking cycle. They are expected to possess high values of strength, hardness and elastic modulus. Additionally, it also has an important influence on the friction and wear properties of the friction material. The properties of the friction material can also depend on the size, shape, geometry, dimensions, concentration and distribution of the fiber reinforcements and their pattern [20]. With respect to reinforcing pattern, fibers are divided into zero dimensional (particles in one plane), one dimensional (long fibres in one plane), and two dimensional fibers (Fibres arranged in two planes). Fibres of different shapes could be used to achieve complex properties or enhance existing property. For e.g: Bond strength between carbon fibres and polymer matrix can be increased by adding zero dimensional fibres [20]. Some of the commonly used fibers (organic and inorganic) for the friction material are shown in table 8.3 below [18].

Fiber Material	Description / Remarks
Aramid	High strength, toughness, hardness High temperature stability, Good thermal and electrical insulation Low density
Glass	High strength Abrasive and Brittle Softens at high temperature High wear
Asbestos	Mineral composed of Mg and Fe silicates High strength and toughness High temperature stability and corrosion resistance Extremely hazardous to health
Barium Sulphate	Inert and stable at high temperatures May aid in wear resistance
Cashew Dust	Improves resilience and reduces brake noise
Lime (CaOH ₂)	Avoid corrosion in Fe additives
Potassium Titanate	Inert filler material; used to replace asbestos
Zinc Oxide	Imparts wear resistance

Table 8.3: Reinforcement/Fiber Materials

8.1.4 Binders

A binder or matrix is essentially a binding and shaping component of a friction material. The properties of the binder determine process conditions for manufacturing and important operating characteristics like working temperature, fatigue strength, resistance to environmental effects, density and specific strength. The table below shows the most commonly used binders [18].

Material	Description / Remarks
Phenolic Resins	common binder; too little - material weakness; Drop in co-efficient of friction at high temperatures due to polymer cross-linking
Alloys of Cu, Fe, Ni	Fe-based metallics have a lower friction response than Cu-based matrix materials
Modified Resins	Used to modify bonding characteristics and temperature resistance Eg: cresol, epoxy, cashew, PVB, rubber, linseed oil

Table 8.4: Binder Materials

8.1.5 Classification of Brake Pads

Many studies [22] [23] [24] [25] have been conducted to understand the constituents by composition. In a number of cases, a range of the percentage of material is reported rather than the exact value (see table 8.5 below). This may be done to conceal the actual composition of materials, as it is confidential. Also, some of the compositions

are given in weight percentage rather than volume percentage. It is suggested that volume percentage is the correct unit of measure for friction material composition rather than weight percentage [26]. Even though the wear rate depends on the material composition, just to get an idea, the average wear rate of an automotive brake pad is 0.5 micrometers per brake application which is approximately 3 mg of material loss [27]. The summary of compositions of a brake pad are shown in table below [18].

Friction Material Constituent	Range (Vol %)
Phenolic Resin	10 - 45%
Barium Sulphate	0 - 40%
Fibers	5 - 30%
Cashew Particles	3 - 30 %
Graphite	0 - 15%
Metal sulphides	0 - 8%
Abrasives	0 - 10%
Friction dust	0 - 20 %

Table 8.5: Friction Material Constituents

The classification of brake pads is generally made based on the friction material constituents used. The table below shows the general classification of brake pads.

Brake Pad Type	Features
Semi-Metallic (ECE)	<ul style="list-style-type: none"> -Contains 30%-65% metal - Made of steel wire or metallic wool, graphite or copper, and friction modifiers - Long- term durability and excellent heat transfer capability - Noisy, high wear rate, low efficiency at low temperatures
Non-Asbestos Organic (NAO)	<ul style="list-style-type: none"> - Made of fibers, high-temperature resins, and filler materials - Softer and create less noise than Semi - Metallic - Deteriorate faster and create more dust
Low Metallic NAO	<ul style="list-style-type: none"> -Contains 10%-30% metal and organic materials - Excellent braking and heat transfer capabilities
Ceramic	<ul style="list-style-type: none"> - Contains ceramic fibers, bonding agents, non ferrous filler materials - Less noise, wear down slowly, create less dust - Expensive

Table 8.6: Brake Pad Classification

8.2 Brake Disc Materials

The mechanical aspects of brake discs are already briefly discussed in section 5.1. Historically, the needs for a braking system was realised in 1886 after the first automobile accident happened. Elmer Ambrose Sperry invented the first brake disc called magnetic brake, similar to what we use today. Two discs were placed on each other to apply a brake torque [28]. The design and the chemical composition of brakes affect the heat flow, the durability, the noise generation, the maintenance ease, and consequently, the performance of brake discs. The working temperature for passenger cars, based on the severity and braking frequency, can be placed between

-40° C to 900° C. This high range creates higher temperature gradients in the disc, which causes thermal fatigue. However, the component is also exposed to a cyclic mechanical load applied by the pads during a braking event, which contributes to the component's wear. Therefore, in real working conditions, the disc is exposed to a thermomechanical fatigue loading condition instead of only thermal [28]. There has been a considerable amount of evolution in the brake disc design during these years like incorporating heat out vents, topology optimization to reduce weight etc. But, much of the evolution has happened in the material design. Let us look at the different disc materials used in automotive brakes today in the upcoming sections.

8.2.1 Cast Iron

Cast iron has been a most common choice of disc material due to a high metallurgical stability, lower cost and ease of production. Cast iron can be classified as: gray, nodular, vermicular, malleable and white. Nowadays, gray cast iron alloys are widely used due to the best price/benefit ratio. During production of the several types of cast iron, the molten raw material usually consists of pig iron (reduced iron ore), scrap iron and alloy elements like silicon, manganese, chromium, nickel, among others. All these alloying elements tend to increase mechanical strength, and the most efficient are vanadium, molybdenum, and chromium. Varying the chemical composition and cooling speed can result in different microstructures like ferritic, ferritic-pearlitic and pearlitic. The table below shows the some improvements in the cast iron disc done over the years [6].

Improvement	Result	Initiated by
Addition of 0.05 wt% of titanium to the cast iron	Helps to bind nitrogen, Wear reduction of 45%	Audi AG, 1990
Adding 0.1%-0.25% of titanium to high carbon cast iron	Improves hardness and reduce wear	Sichuan Vanadium & Titanium Brake Ltd., 2014
Addition of 1.5 wt% of molybdenum to cast iron	Increased wear resistance	Piwowsky, 1942
Addition of 0.1-0.3 wt% niobium to high carbon cast iron	High temperature strength and high wear resistance	Shandong Hong MA, 2014
Incorporating a sealing between cast iron base and protective layer	Improved wear resistance	Meyer and Lambach, 2012
Surface hardened by ceramics of thickness 2-5mm on rubbing ring	Enhanced life by a factor 4.6	Qihong, 2011
Dual coat concept: Coating on rubbing ring and the rotor hat	Enhanced wear resistance and corrosion prevention	Keith, 2009

Table 8.7: Evolution in Cast Iron Disc Material

8.2.2 Aluminum Composites

Although cast iron brake discs have many advantages, other materials for the base body have become interesting for automotive applications during the last 20 years. Brake discs made of aluminum based metal matrix composites (Al-MMC) might represent one possibility for future brake systems. Al-MMC consists of Aluminum silicate ($AlSi_2O$) with 15-25 wt% of silicon carbide. Spray-forming process can be used to apply additional hard material particles made of Al_2O_3 , SiO_2 , TiO_2 , SiC , tungsten carbide, boron carbide, titanium nitride, and

Table 8.8: Evolution in Aluminum Composite Discs (Al-MMC)

Improvement	Result	Initiated by
Adding Al ₂ O ₃ , SiC or SiN ₄ in 3~20 wt% hypereutectic silicon alloy.	Excellent abrasion resistance	Hino & Miyashita, 1984
Steel layer on top of Al base disc body	Improved wear resistance, corrosion resistance, and thermal stability	Sichuan Vanadium Titanium Brake Ltd., 2014
Ceramic coating on the braking surface of thickness 0.38-0.5mm	Increased thermal stability as coating acts as heat deflector	Smolen, 1991

titanium diboride. In total the amount of hard material particles is around 45 wt%. The table below shows the some improvements in Al-MMC done over the years [6].

Al-MMC is not only used to reduce weight and minimize the mechanical wear, however this material is not resistant to high temperatures [6]. That is the reason behind using them only on the rear wheels rather than the front where braking torques and temperatures are high [28]. Even though there are serious performance issues, originally it was assumed that there would be reductions in brake noise but that is not the case. Comparison of sliding wear performance between Al-MMC and cast iron discs against organic and semi metallic brake pads show that friction and wear of Al-MMC was high at high speeds and loads. But, it could be greatly improved if the pad and disc combination is chosen properly. For example: Organic pads were a better match to Al-MMC than the semi metallic pads. Finally, it can be stated that discs made of aluminum, especially Al-MMC concepts, may represent a very promising approach to reduce brake wear and particle emissions.

Even if doubts are cast on parameters such as the critical temperature limit of around 400° C and the material and manufacturing costs are unanswered so far, Al-MMC disc concepts will become more relevant in the future. The introduction of hybrid, full-electric and self driving vehicles to the markets might help overcome the drawback of low temperature limits because regenerative braking will lead automatically to much lower operating temperatures.

8.2.3 Ceramics

Ceramic composite brake discs, mostly just called ceramic brake discs, could be the ideal material candidates for reducing wear and PM emissions. Originally designed for high-performance applications, this type of brake discs have also shown a significantly better wear performance because of high hardness. The material design is such that, they have a multi layer structure consisting of carrier bodies and friction layers, both reinforced with carbon fibers. Despite of efforts to improve the manufacturing processes of ceramic brake discs, production is still very time and energy-consuming with lower operational efficiency compared with that of cast iron discs, which leads to significantly higher costs [6].

Improvement	Result	Initiated by
Carbon to reduce fiber content or even replace them entirely	Reduces wear and helps generate friction film	Kienzle and Kratschmer, 2007
Machining the carbon fiber reinforced disc brakes such that Ra is less than 2.5 microns.	Reduced wear and higher friction	Johnson ,2009
Continuous fibers arranged at an angle of 60° in radial direction	Reduces fiber pullout and wear	James, Murdie and Walker, 2002

Table 8.9: Evolution in Ceramic Discs

In conclusion it can be stated that ceramic brake rotors represent an interesting alternative to reduce PM emissions and wear from the technical point of view, but the costs are still much higher and it is expected that ceramic brake discs will be used in the future only in unique applications such as sport cars.



9 Material Wear Mechanisms

PM resulting from non exhaust emissions is due to brake, tire, and general vehicle wear. Several studies have shown that the automotive brake wear is the highest PM contributor compared to other non exhaust emission sources. Since wear is the root cause of brake PM emissions, the wear phenomenon and different wear mechanisms will be discussed in this section.

Wear is defined as the continuing loss of material from the surface of a solid body due to mechanical action i.e. contact and relative movement of a solid, fluid or gaseous counter body. A wear coefficient is a physical coefficient used to measure, characterize and correlate wear of materials. It is denoted by K .

$$K = \frac{\text{Wearvolume} * \text{Hardness}}{\text{Load} * \text{Slidingdistance}}$$

The amount of wear is dependent on the Material hardness, applied normal loads and sliding distance. So, for a given drive cycle if two materials are tested, then wear should be completely dependent on material hardness as the load and sliding distance remain constant. But, that is not the case since a friction material is a composite material consisting of at least 10 different compounds. These organic and inorganic compounds are powdered, mixed together and compacted with some thermal treatment after which the friction material or the brake pad is ready to be used. There are some defects during manufacturing like pores, inclusions etc. that affect wear rate.

9.1 Classification of wear

During a braking event, the friction material is exposed to high thermo mechanical loads which leads to 2 distinct types of wear. They are:

1. Wear dominated by mechanical wear of materials
2. Wear dominated by chemical wear of materials

Further, the sub classification of wear types, and their causes and effects are shown in table 9.1 [29] [30] [31].



	Wear Type	Cause	Visual identification
Mechanical	Abrasive wear	Abrasion between two contact surfaces and removal of material surface	Hard glassy phase, irregular mineral chips, larger mineral fragments
	Adhesive wear	Contact interface between two surfaces under plastic contact has enough adhesive strength to resist relative sliding	Shear of ductile materials & transfer of material to counter surface
	Plowing wear	Similar to abrasive wear	Groves on the surface, large areas of resin matrix
	Particle Pullout	Improper compaction between fibers and matrix	Brittle constituents of irregular shape, mineral fragments
	Fatigue wear	Wear generated after repeated contact cycles	Peeling of mineral layers followed by fracture
Chemical	Corrosive wear	Reaction products formed by interaction of surface and corrosive environment	Growth of an additional layer on surface
	Diffusion wear	Due to heat produced during continuous frictional contact between 2 surfaces	Degradation of the surface.

Table 9.1: Types of Wear

9.2 Brake Pad Wear

Having discussed about the general wear mechanisms, let's look at how the wear happens in a friction material during braking event. The friction and wear behaviour of automotive brakes is determined by the characteristics of the active surface between the pad and the disc and the third body layer formed between these surfaces [23]. The brake wear mechanism happens in 3 steps:

1. Formation of Friction Layer
2. Development of Contact Plateau
3. Wear

9.2.1 Formation of Friction layer

When the brake pad and the disc rub against each other during a braking event, at first there is abrasive wear which creates friction debris between the surfaces. Later, this debris adheres to the friction surface of the brake pad which results in the formation of a friction layer [6]. The formation of the friction layer is directly proportional to the speed, temperature and brake energy. So, as the braking frequency increases there is abrasive/ploughing wear which creates long grooves on the brake pad which in turn will be filled with wear debris over the braking cycle forming a thick friction layer.

9.2.2 Development of Contact Plateau

Microscopically, there is a complex contact situation [23]. Unevenly distributed wear and compaction of wear debris results in a surface characterised by flat plateaus rising above the rest of the surface. There is a formation of primary and secondary plateaus. The primary plateaus consist of the wear resistant components of the pad and act as nucleation sites for the secondary plateaus. A maze of grooves are formed between the pad and disc due to the frequent contact between the moving disc and the debris, in the form of minute particles.

Intermittently, this debris builds up against the primary plateaus. The normal brake pressure, shear forces and the friction heat results in the compaction of the debris, forming secondary plateaus. The plateaus can be spotted on the brake pads as shiny spots against a dark background. So, in order to form a secondary plateau, wear debris is very much required coupled with the increase in pad-disc space. This can only happen when several braking events are done and that is the reason why secondary plateaus are formed at a slower pace compared to primary plateau [23]. That is why it is believed that the brake pad performance increases after the burnishing cycle (see section 10.2).

9.2.3 Wear

Generally, wear of any material happens when the applied load on the material exceeds the strength of the material. So, in case of a brake pad, wear happens when the contact plateaus fail. In situ studies have shown that secondary plateaus require primary plateaus for structural stability. The hardness and the strength of the contact plateau containing primary and the secondary plateau shows that the overall strength of the contact plateau is dependant on the primary plateau which is made of fibers. Hence, the depth of the primary plateaus is much higher than the secondary plateaus. Micro scratching reveals that secondary plateau have higher compressive strength compared to tensile strength [32]. Hardness of the secondary plateau is much lower than the primary plateau. Nanoindentation of secondary plateau shows that the hardness values vary between 0.2 and 4GPa, depending on indentation depth. This means that the higher hardness value is contributed by the friction layer which is 50 nm deep approximately [23]. The secondary plateau degrades in milliseconds after the primary plateau and friction layer fails due to the shear forces acting during a sliding contact.

10 Methodology

In this section, the method of experimentation will be discussed in detail. An overview of the test bench setup at Volvo Cars and instruments as well as methods used for measurement will be described. The goal of the experiments was to measure particles being emitted by various brake pad and disc combinations in a realistic, every-day braking cycle.

10.1 Test Setup

10.1.1 Overview

The test setup for the particle measurement experiments was designed based on the availability of instruments and test bench features at Volvo Cars. The test bench used was a brake dynamometer (dyno), as has been used in many of the brake particle measurement experiments conducted previously, discussed in section 6.3.1. The brake dynamometer at Volvo Cars is used for simulating the load of a vehicle and the braking torque, or force—it consists of a shaft connecting a fixture where a brake disc can be mounted to a rotating mass representing the inertia of a vehicle. This can be seen in the side view of the test setup in Figure 10.1. The programming and outputs of the dyno will be discussed further in section 10.1.2.

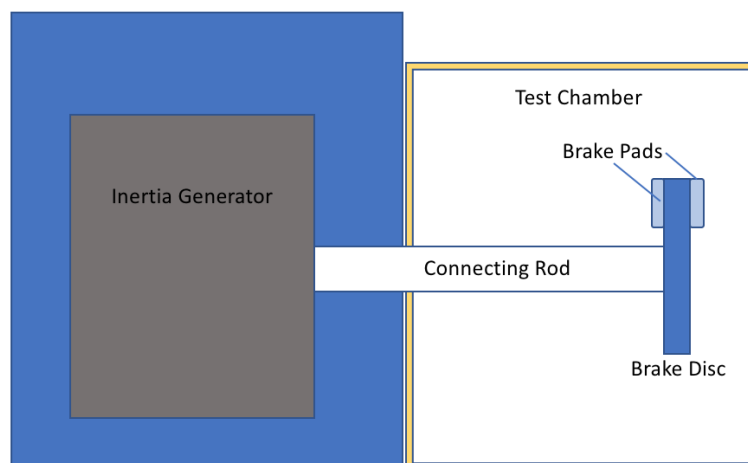


Figure 10.1: Side View of Brake Dyno Test Setup

In order to assure that the experiments would allow the proper measurements and analysis, various departments were consulted for using equipment and seeking suggestions for testing. The Department of Air Quality provided the particle mass and count measurement device- an Electrostatic Precipitator (ESP) discussed further in section 10.1.3, while the Exhaust Department was able to provide a filter for collection of the particles in the chamber, discussed further in section 10.1.4, so the particles could be analyzed under the scanning electron microscope (SEM) afterwards. The locations of the testing points for the ESP and particle filter in the chamber are shown in Figure 10.2. In terms of insight, particle experts from the Environmental Attribute and Material Management Department and the Research Institute of Sweden (RISE) were consulted regarding the toxicity of particles depending on their size, shape, and material, as well as for advice with respect to operating particle measurement devices.

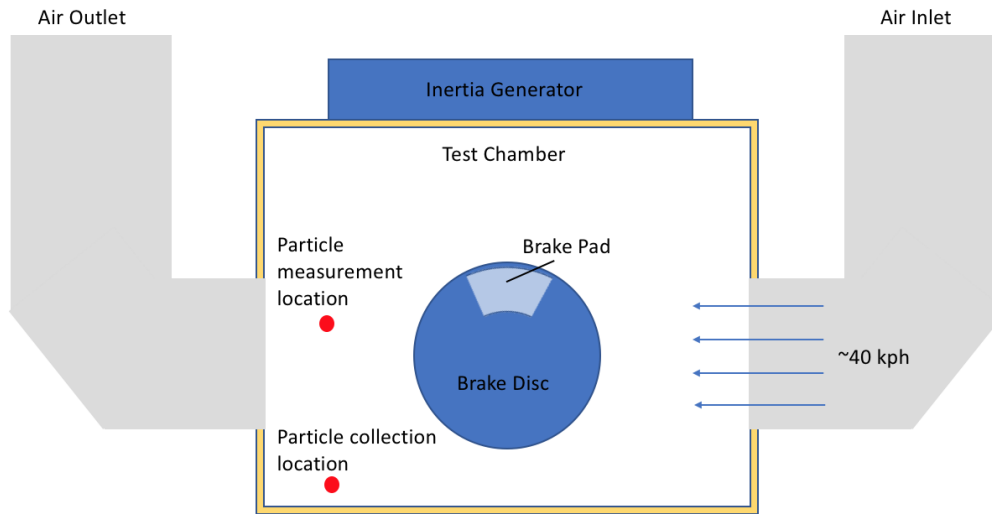


Figure 10.2: Front View of Brake Dyno Test Setup

10.1.2 Brake Dynamometer

As mentioned above, the brake dynamometer at VCC used for the experiments in this thesis is used to simulate the inertia of a vehicle. The magnitude of the inertia can be adjusted to represent different sized vehicles. In this case, an inertia of $66\text{kg}\cdot\text{m}^2$ was used, equivalent to that of a S60—a common, average-sized sedan. In addition to the simulated inertia, the size of the brake disc, and the corresponding caliper and brake pads must be changed in order to match with the desired vehicle model. In the case of these tests, a standard front-axle seventeen inch grey cast iron brake disc was used to match with the $66\text{kg}\cdot\text{m}^2$ inertia, and the brake pads were changed in order to compare the particle emissions created by different brake pad materials. The dyno has the ability to be mounted with many different sized disc brakes.

Before running PM emissions test using the brake dynamometer, it was imperative to know the source of the airflow through the chamber, because as can be seen in Figure 10.2, an airflow through the chamber is used to simulate real-world driving conditions. (The air speed of 45 km/h was selected in correspondence with the selected driving cycle which will be explained in section 10.2.) It was confirmed that the air source is taken from the roof of the building through a large filter, and this was acceptable for the experiments at hand.

The brake dynamometer uses a program to run braking cycles designed by the user. These braking cycles can be defined by many different parameters, some examples being: magnitude of deceleration, brake pressure, braking time, or brake disc temperature. The braking cycles used for this thesis are discussed further in section 10.2.

10.1.3 Electrostatic Precipitation Particle Measurement

The previous studies done at VCC internally, mostly used impactors in order to measure and/or collect particles. However, the only low-pressure impactor at VCC is too large to be feasibly used in the brake dynamometer. Therefore, as mentioned previously, the particle measurement device used for these experiments was an electrostatic precipitator which was provided from the Department of Air Quality at VCC. An electrostatic precipitator

(ESP) is an instrument which uses the phenomenon of electrostatic precipitation to collect the particles flowing in a stream of gas. The electric charge supplied to the particles forces them to pass through a corona (gaseous ion flow region). The electric field for the particles comes from the electrodes maintained at high voltage in the center of flow path.

This device is able to measure the particle size distribution and particle mass distribution in real time, meaning the count of particles and the total mass of particles per unit volume, and sorted by the size of the particles measured by their aerodynamic diameter. The ESP has 41 size-categorized channels ranging from aerodynamic diameters of 10nm to 35 μ m, so the output measurement is the count and mass of particles in each of these 41 categories. That being said, it is important to note that the ESP is a device meant for measuring very small particles.

Using the electrostatic precipitator to analyze particle distribution is done best when the airflow collected from the sampling tube is low-speed and isokinetic. This posed a challenge with the test setup in the brake dynamometer, as the conditions were assumed to be turbulent and nonuniform in the test chamber. For this reason flow meter tests were run to characterize the flow in the chamber and determine the best location for placing the inlet sampling tube for the ESP. Figure 10.3 shows the different sampling locations.

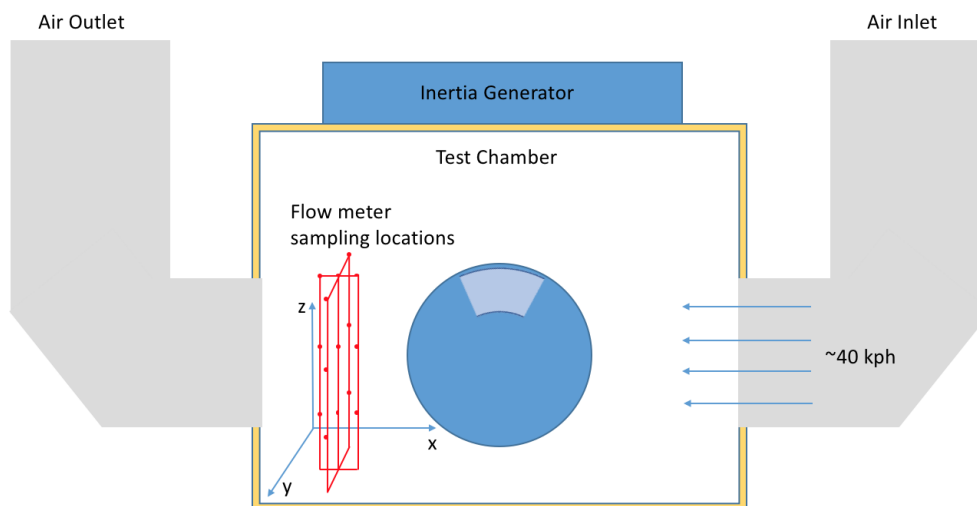


Figure 10.3: Flow Meter Test Locations in the Dyno Test Chamber

From these airflow sampling tests, the sampling location was chosen taking into consideration the average speed and standard deviation. With respect to the x and y axes, there was not a big difference in the standard deviation and air speed. However, on the z axis there was a large gap in stability and speed between the air at the top point and the lower two points. Thus, the top location was ruled out due to turbulence, and it was decided to run the tests at middle position, at a height of 50cm. The middle height was chosen to rule out the possibility of having particles that would otherwise settle on the bottom of the chamber as sediment, go into the sampling tube from the position that was closer to the dyno floor.

With regards to the output measurement of the ESP, it is important to note that the data output frequency of the machine is 0.0167 Hertz. This was problematic due to the fact that the dynamometer has a measurement frequency of 0.2 seconds, and the average duration of a braking event in the WLTP cycle is 5.7 seconds. Thus, when overlaying the dynamometer and ESP data, it was considered how to best show the correlation in these

datasets considering the difference in sampling time. This will be discussed further in chapters 11 and 12.

10.1.4 Particle Capture Equipment

One of the important aspects of the study was to collect the PM emission and analyze the particles to understand the toxicity of the elements. Many candidates were considered like the Volvo Cabin filter, High efficiency particulate air (HEPA) filter and a polymer based filter. Although the cabin filters and HEPA filters were better choices, mounting them in the chamber was a challenge. The filter finally used in the experiment was a membrane type polymer filter made by Pallflex. Filter is made of Borosilicate glass microfibers reinforced with woven glass cloth and bonded with Poly tetra fluoro ethylene (PTFE). Typical applications of this filter lies in measuring exhaust particulate matter PM1, PM2.5 and PM10. Since this filter could only be placed in the bottom of the chamber, some sort of suction pressure was needed to be able to collect particles. The filter was connected to the pump with the suction pressure set at 0.7bar, just less than the atmospheric pressure so that we:

1. Simulate the human breathing conditions
2. Avoid disturbances in the airflow which may affect particle flow

10.2 Dynamometer Test Cycles

As mentioned previously, the dynamometer must be programmed to perform a desired braking cycle. Most testing done in the brake dynamometer begins with a burnishing cycle—consisting of 30 stops at a pressure of 30 bar each from an initial linear speed of 80km/h to 30km/h, shown in Figure 10.4. This is equivalent to the burnishing that is done on the brake discs of vehicles before they are ready to be driven for the first time. Therefore, the burnishing cycle was run on each of the new discs initially before a braking cycle.

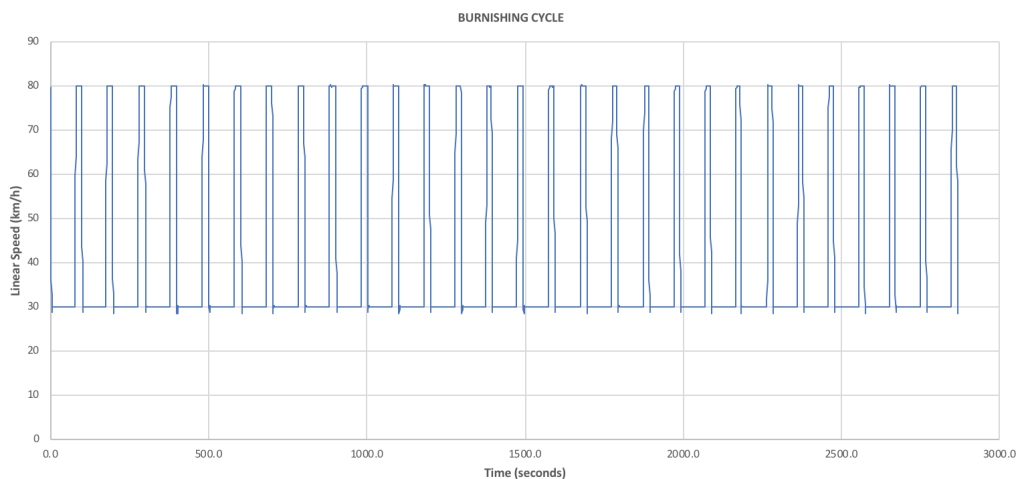


Figure 10.4: Burnishing Cycle Speed Profile

In a joint research between Ford and the European Commission, braking patterns were analyzed in order to develop a braking cycle that is representative of real-world driving conditions, and therefore representative of

the emissions caused by braking during "real-world" driving. This braking cycle that was developed is called the Worldwide Harmonized Light Duty Vehicles Test Procedure (WLTP) cycle [33], and is the braking cycle that was used for the experiments conducted in this thesis. The idea behind the development of this braking cycle was to obtain a universal methodology for the measurement of braking particle emissions.

During the research done to develop this cycle, over seven hundred thousand kilometers of driving data was recorded in five prominent driving regions: Europe, the United States, India, Korea, and Japan, and across the regions it was found that the braking frequencies were similar. However, for the statistics, the European portion of the WLTP database was used to replace that of India, Japan, and Korea since the vehicles in those regions were being operated by instructed drivers opposed to the more realistic case of customer data collected in Europe. Many parameters such as brake event duration, brake event distance, magnitude of deceleration, starting velocity, and number of brake events per kilometer, were considered in the shaping of the WLTP braking cycle [33].

The WLTP braking cycle has 303 braking events over the course of 192km. During the cycle, the average speed is 43.7 km/h, close to the average of the database at 46.5 km/h and, as seen below in Figure 10.5, the top speed reached is 132.5 km/h. The deceleration values vary from 0.05g's (0.49m/s²) to 0.22g's (2.18m/s²) [33].

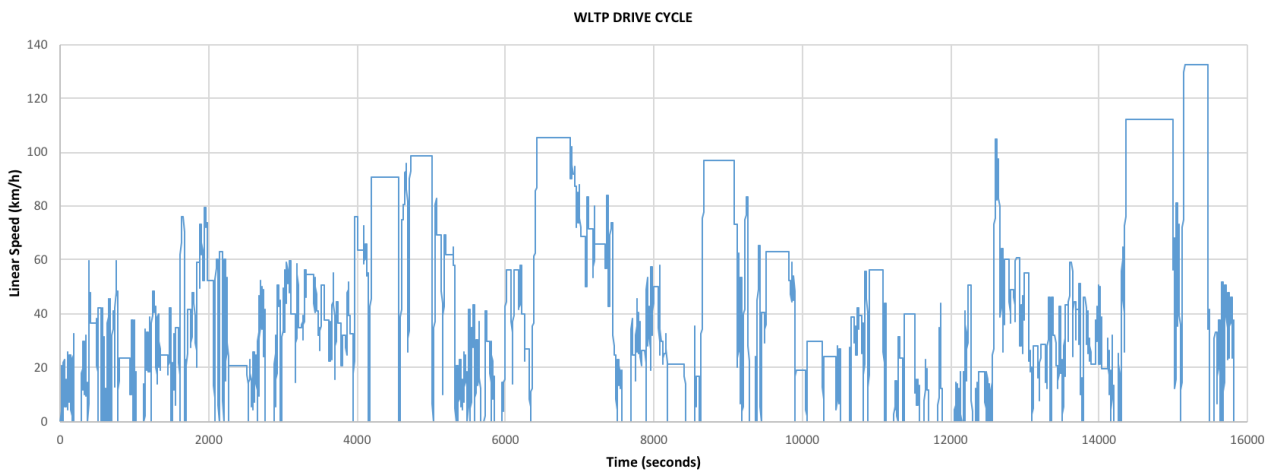


Figure 10.5: WLTP Novel Brake Cycle Speed Profile

When compared to other driving cycles, such as the Los Angeles City Traffic (LACT) Cycle, the WLTP Cycle is quite mild with respect to braking and deceleration, which is supporting the idea that brakes are used conservatively in a majority of cases. This brake cycle was chosen for this thesis in order to have the possibility to compare results in the future once the WLTP Cycle is universally adopted as a standard cycle for measuring braking emissions. Using this braking cycle will make the data useful for future studies, further discussed in chapter 14.

This WLTP cycle was developed for internal combustion engine (ICE) vehicles, in other words, vehicles that do not use regenerative braking and rely solely on friction braking for deceleration. However, a braking cycle was needed to simulate the friction brakes applied in an electric vehicle. As discussed in section 7.2, the friction brakes are only needed a fraction of the time in an EV as compared to an ICE vehicle. In order to simulate the same sort of braking pattern for an electric vehicle, a conservative, general estimation was applied to the WLTP cycle by assuming that an electric vehicle would need 30% of the magnitude of the braking events as compared to an ICE and that 70% of the braking energy was accounted for by regenerative braking at all speeds

and we call it WLTP EV cycle. So the magnitude of deceleration in each of the 303 stops in the WLTP cycle was multiplied by 0.3 as seen in Equation 10.1:

$$decel_{WLTP,EV}\left(\frac{m}{s^2}\right) = 0.3 * decel_{WLTP,ICE}\left(\frac{m}{s^2}\right) \quad (10.1)$$

The source of this estimation value is from internal sources at Volvo Cars Corporation.

10.3 Experimental Test Plan

The tests to be run were decided based on the main purposes of this thesis: to compare the particle emissions coming from different material brake pads, analyze how electrification of the automotive industry and regenerative braking will affect particle emissions of brakes, and furthermore how particle emissions are affected by corroded brakes. Since the targeted market for this analysis is Europe, the baseline experiment was the ECE brake pad and GCI brake disc run with the WLTP Cycle meant for an ICE vehicle. The other two brake pad materials tested for comparison were NAO pads (commonly used in the US and China markets), and a new NAO pad that has been designed to decrease particle emissions provided by one of VCC's suppliers, also both run with the WLTP Cycle meant for ICE vehicles. Then, the baseline experiment using ECE pads and GCI disc was run using the WLTP EV Cycle to simulate the braking of an electric vehicle. Lastly, all four tests discussed were run again after placing the brake disc in a corrosion chamber overnight to replicate a brake disc left on a vehicle and not driven over the weekend. The eight tests run are summarized in table 10.1.

Test Number	Pad Material	Braking Cycle	Corrosion Status
Test 1	ECE	WLTP ICE	plain
Test 2			corroded*
Test 3	NAO	WLTP ICE	plain
Test 4			corroded*
Test 5	New NAO	WLTP ICE	plain
Test 6			corroded*
Test 7	ECE	WLTP EV	plain
Test 8			corroded*

Table 10.1: Tests Conducted

* The results for the corroded tests are not included for PM emission plotting. This is due to the fact that Test 2 and Test 4 were run with a burnishing cycle prior to the WLTP cycle, which was erroneous. The burnishing cycle and its heavy braking applications most likely got rid of most of the rust particles on the surface of the disc before the WLTP cycle was run. Therefore these results cannot be compared with the original ECE and NAO tests- Test 1 and Test 3.

10.4 Ranking Parameters To Be Measured

Before the tests were run, some key parameters were identified that should be used to rank the brake pad materials with respect to particle emissions, quality, and safety.



- Particle Size Distribution by Mass (PM1, PM2.5, PM10 in $\mu\text{g}/\text{m}^3$)
- Particle Size Distribution by Count (PM1, PM2.5, PM10 in count of particles/ cm^3)
- Materials Present in Emission Particles
- Total Mass Lost (weight and thickness of disc and pads before and after test)
- Maximum Disc Temperature Achieved During Cycle



11 Results

11.1 PM Emissions

The results in this section will be displayed showing the PM emissions with respect to mass and count overlaying the speed profile of the cycle. Since the measurement frequencies of the ESP and brake dynamometer were so different, it was found that this is the best way to show the correlation between PM increases in the air and braking events. The most noteworthy trend in these plots is the correlation between peaks in PM emissions coinciding with braking events performed at higher speeds.

ECE Pads

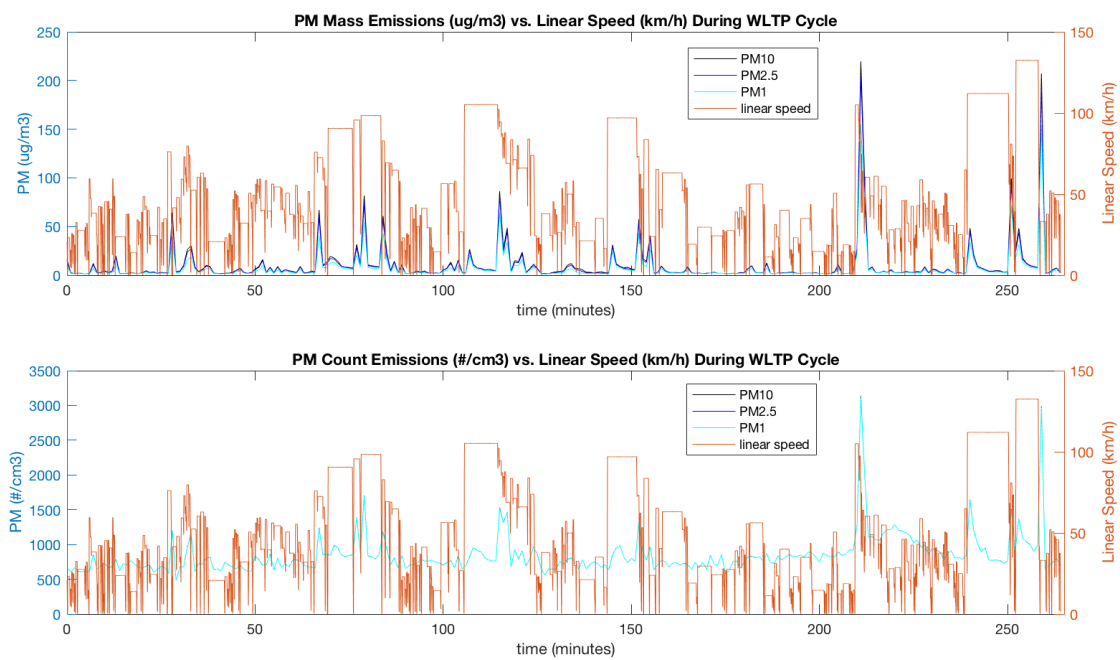


Figure 11.1: ECE Pads Linear Driving Speed Profile vs. PM Emissions

NAO Pads



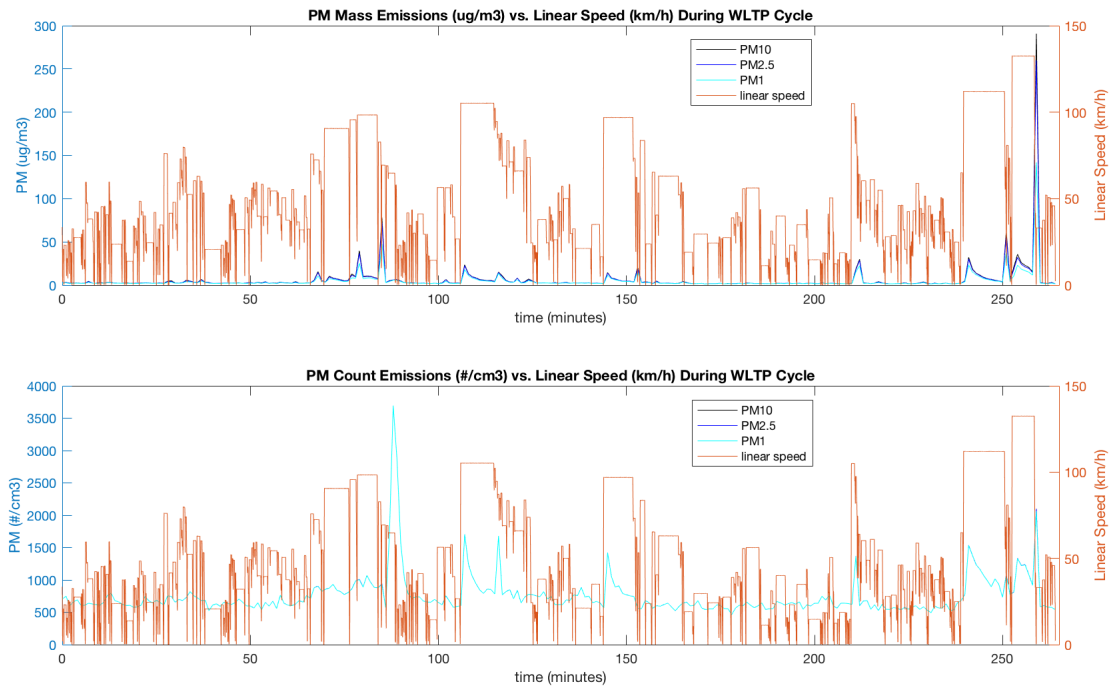


Figure 11.2: NAO Pads Linear Driving Speed Profile vs. PM Emissions

New NAO Pads



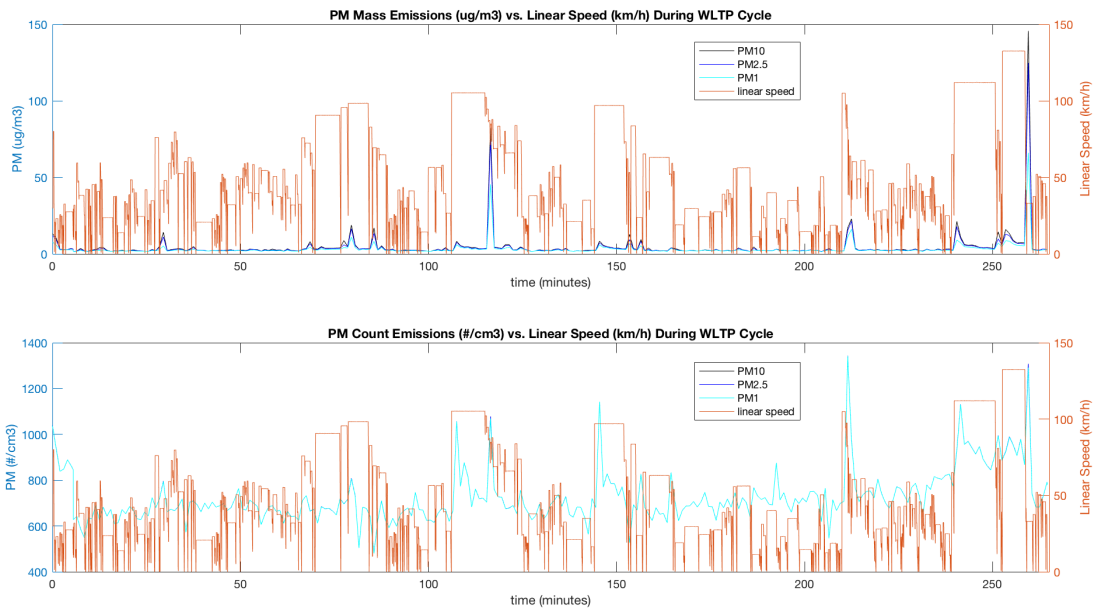


Figure 11.3: New NAO Pads Linear Driving Speed Profile vs. PM Emissions

ECE Pads with EV Cycle

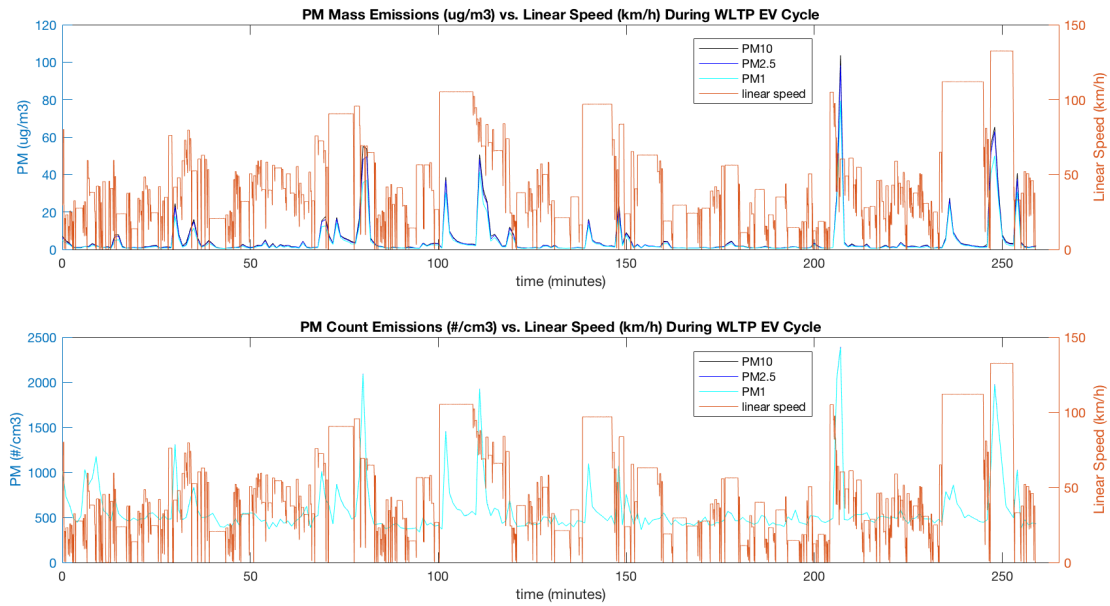


Figure 11.4: ECE Pads with EV Cycle Linear Driving Speed Profile vs. PM Emissions

Something else important to note in the measurement of particles is the difference between mass and count measurements. It is extremely imperative to measure both, since the particles of PM1 contribute much less to the particle mass than to the count. For example, one particle of size PM10 can contribute as much to the mass measurement as at least hundreds of nano-particles combined. Therefore, it is seen in the results that a majority of the particle count is PM1, while PM2.5 and PM10 are comparatively hard to see in terms of count, however, these few particles of PM2.5 and PM10 are clearly represented in the results of mass measurement. Another important observation in these plots is the signal-to-noise ratio. It is clear that there is a background level of PM1 particles present in all of the experiments, most prominently observed in the plots for PM count emissions. In the PM Count plots, there is a significant background level of PM1 particles even when there are no braking events occurring for several minutes. Since these particles are so small however, the background noise is not so evidently seen in the PM mass plots. Quantifying this background noise of particles is discussed further in section 14.

11.2 Brake Disc Temperature

As mentioned previously, the measurement frequency of the ESP is once per minute, while the brake dynamometer is five times per second, and many of the braking events are only several seconds long. Therefore, the PM emission data may be lagging a bit in response to a braking event, and thus, the average disc temperature over each minute was calculated in order to see if a higher average disc temperature from the previous minute would correspond with an increase in PM emissions for that minute. This trend proved to be true in some cases, as can be seen in Figure 11.5.

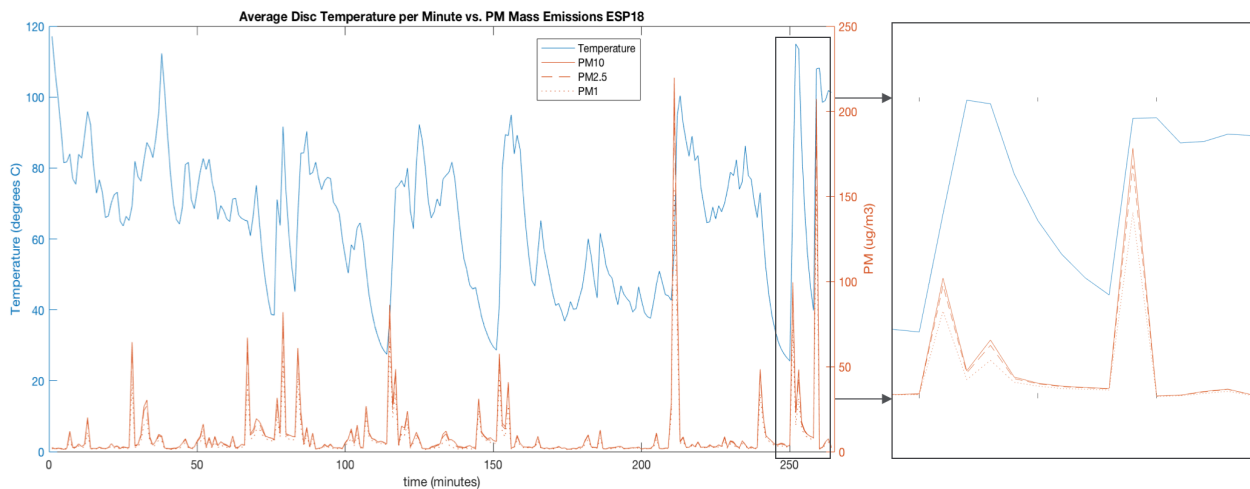


Figure 11.5: Average Disc Temperature in 1-minute Intervals vs. PM Emissions for ECE Pads

But that being said, this experiment was not designed to show the relationship between temperature and PM emissions. Since the WLTP braking cycle was very mild, the disc temperatures reached were not very high. The relationship between quantity of particles and temperature is usually seen at disc temperatures above 200 degrees Celsius [13]. The maximum disc temperatures across the entire WLTP cycle for each of the tests is summarized in table 11.1.

Pad Material	Maximum Disc Temperature
ECE Pads	135.5°C
NAO Pads	139.2°C
New NAO Pads	134.3°C
ECE Pads EV Cycle	111.9°C

Table 11.1: Maximum Disc Temperatures Achieved in WLTP Cycle for 3 Brake Pad Materials

As can be seen above, the temperatures are quite similar during the cycles for all three materials. Though the NAO pads seem to have caused the highest brake disc temperature, PM emissions were not higher for this brake pad. However, at temperatures this low and very mild braking events, it is expected that disc temperature will not greatly affect the PM emissions.

11.3 Wear Measurements

The basic purpose of making wear measurements was to understand the amount of wear and the nature of wear on the brake pads. There were totally 8 tests conducted comparing 3 different materials. To have a good comparison, it is necessary that the tests are conducted uniformly with same test cycle. But, since the test cycle was abruptly stopped while conducting the test 6, the wear is not uniform. Due to this we will be unable to compare the wear measurements on New NAO pads. Nevertheless, we will be able to compare:

1. ECE and NAO pads tested with ICE cycle
2. ECE pads tested with ICE and EV cycle

The wear measurements done in this thesis are:

1. Thickness and Weight measurements- To understand amount of wear
2. Flatness profile measurements- To understand the nature of wear

11.3.1 Thickness and Weight Measurements

The main purpose of measuring the thickness and weight before and after the tests was to understand the amount of wear. The amount of wear should have a direct correlation with the PM emission. The thickness was measured across three locations on the pad and the disc. The tables below showcase the results.

Thickness Measurements

1. ECE v/s NAO pads (tested with ICE cycle)

Test Type	Pad/ Disc	Before (mm)	After (mm)	%Decrease in Thickness	Remarks
ECE	Outer Pads	17.21	16.96	1.45	Bad (More wear)
	Inner Pads	17.20	17.00	1.16	
	Disc	28.00	27.95	0.18	
NAO	Outer Pads	17.24	17.22	0.1	Good (Less wear)
	Inner Pads	17.23	17.08	0.8	
	Disc	28.00	27.99	0.036	

Table 11.2: ECE vs. NAO Thickness Measurements (ICE cycle)

2. ICE cycle v/s EV cycle (tested with ECE pads)

Test Type	Pad/ Disc	Before (mm)	After (mm)	%Decrease in Thickness	Remarks
ICE cycle	Outer Pads	17.21	16.96	1.45	Bad (More wear)
	Inner Pads	17.20	17.00	1.16	
	Disc	28.00	27.95	0.18	
EV cycle	Outer Pads	17.21	17.12	0.52	Good (Less wear)
	Inner Pads	17.21	17.09	0.7	
	Disc	28.00	27.97	0.11	

Table 11.3: ICE vs. EV Cycle Thickness Measurements (ECE Pads)

Weight Measurements

1. ECE v/s NAO pads (tested with ICE cycle)

Test Type	Pad/ Disc	Before (gm)	After (gm)	Weight loss (gm)	Remarks
ECE	Outer Pads	447.80	444.31	-3.49	Bad (More weight loss)
	Inner Pads	463.32	460.41	-2.91	
	Disc	9811.2	9810.9	-0.3	
NAO	Outer Pads	439.78	439.03	-0.75	Good (Less weight loss)
	Inner Pads	449.82	449.07	-0.75	
	Disc	9810.5	9810.9	+0.4	

Table 11.4: ECE vs. NAO Weight Measurements (ICE cycle)

2. ICE cycle v/s EV cycle (tested with ECE pads)

Test Type	Pad/ Disc	Before (gm)	After (gm)	Weight loss (gm)	Remarks
ICE cycle	Outer Pads	447.80	444.31	-3.49	More Pad wear Less disc wear
	Inner Pads	463.32	460.41	-2.91	
	Disc	9811.2	9810.9	-0.3	
EV cycle	Outer Pads	447.59	446.37	-1.22	Less Pad wear Gain in disc mass
	Inner Pads	463.27	462.03	-1.24	
	Disc	9821.1	9835.1	+13.9	

Table 11.5: ICE vs. EV Cycle Weight Measurements (ECE Pads)

11.3.2 Flatness Profile Measurements

Flatness profile measurements were taken for all the brake pads in order to understand the nature of wear. The measurements were taken at the Measurements lab at Volvo Torslanda PV. The nature on both inner and outer pads followed the same pattern in all cases. The figure below shows the flatness profile measurements for ECE and NAO pads (Test 1 to Test 4).

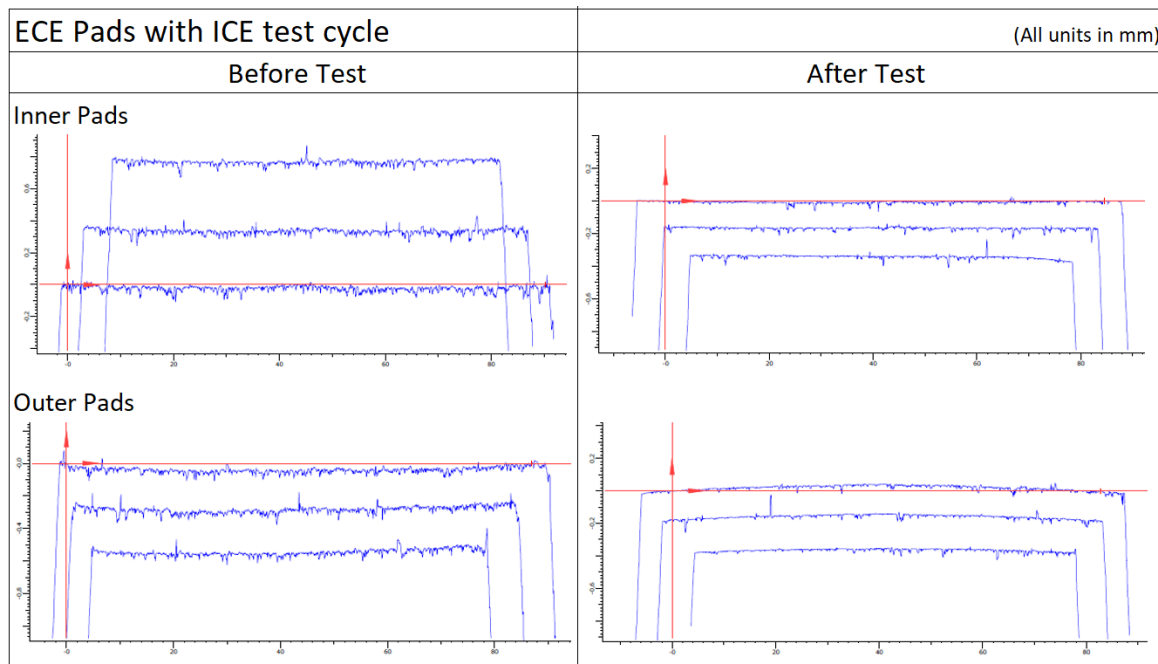


Figure 11.6: Flatness profile measurements for ECE pads tested with WLTP ICE

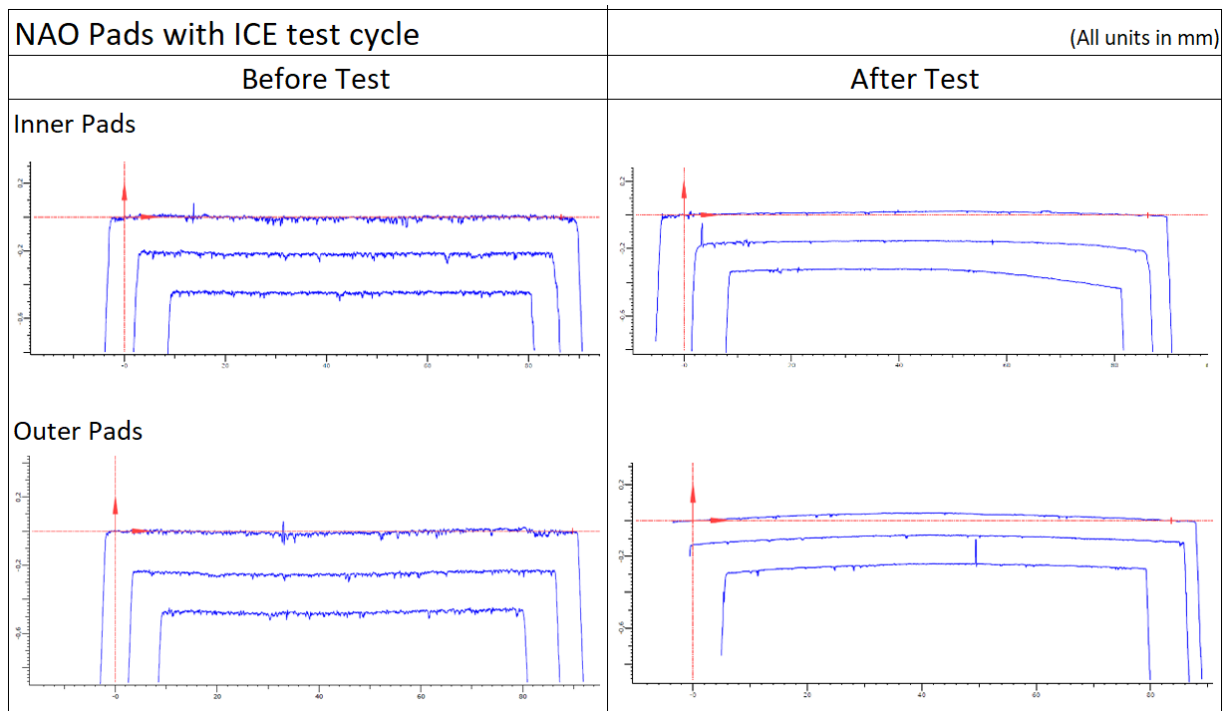


Figure 11.7: Flatness profile measurements for NAO pads tested with WLTP ICE

11.4 Scanning Electron Microscopy (SEM) and Energy dispersion spectrum (EDS) analysis

Several toxicological studies have suggested that metallic brake wear particles biologically cause oxidative stress (see section 6.1) [6] [15]. Therefore, to understand the toxicity of these particles it is important to not only study particle mass, but also the particle quality (e.g. chemical composition and biological effect). An effort was made to collect air borne particles using a filter. Also, the brake pad surface was studied to understand the elemental composition which could shed some light on the toxicity.

11.4.1 Filter analysis

As planned, a polymer based filter was used to capture non-exhaust emissions. The filter was designed for 0.7 bar pressure and operating temperature is 260° C. The particles were collected across the 4 tests conducted.

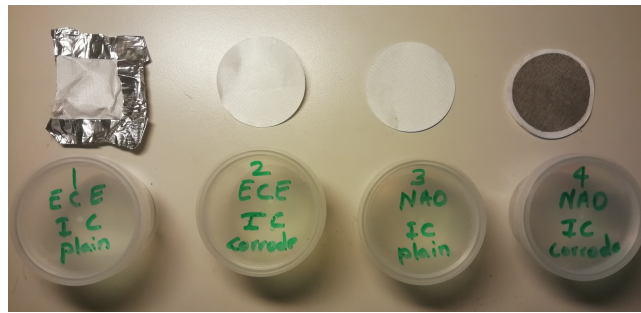


Figure 11.8: Filters for 4 tests after particle collection

The method of analysis chosen was SEM coupled with EDS for which we had an easy access to. Initially when the first sample was mounted, it was difficult to look at the particles as the filter was polymer based and so the conduction was minimal. In order to increase the conductivity, the filter sample was sputtered with 6 nm of carbon. When the SEM was operated at low vacuum condition, we did notice movement of particles. So, the setting was changed to high vacuum to get better particle images. This was followed by the EDS analysis. The analysis results and the SEM images are shown below:

1. ECE pads filter (Test 1)

Element	% Mass
C	20.5
O	28.43
Na	3.25
Mg	0.65
Si	32.93
K	5.11
Ca	9.13
Total	100

Table 11.6: Particle from ECE pads (ICE cycle) captured on the filter

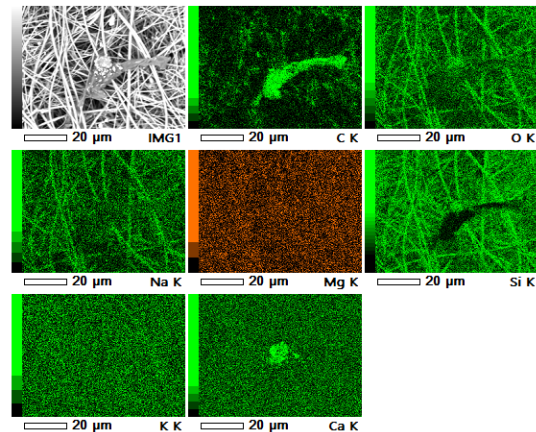


Table 11.7: EDS spectrum of ECE particles captured on the filter

2. NAO pads filter (Test 2)

Element	% Mass
C	13.51
O	18.74
F	14.51
Na	2.28
Mg	0.62
Al	3.51
Si	27.08
K	3.61
Ca	7.33
Ti	0.69
Zn	1.10
Ba	7.03
Total	100

Table 11.8: Particle from NAO pads (ICE cycle) captured on the filter

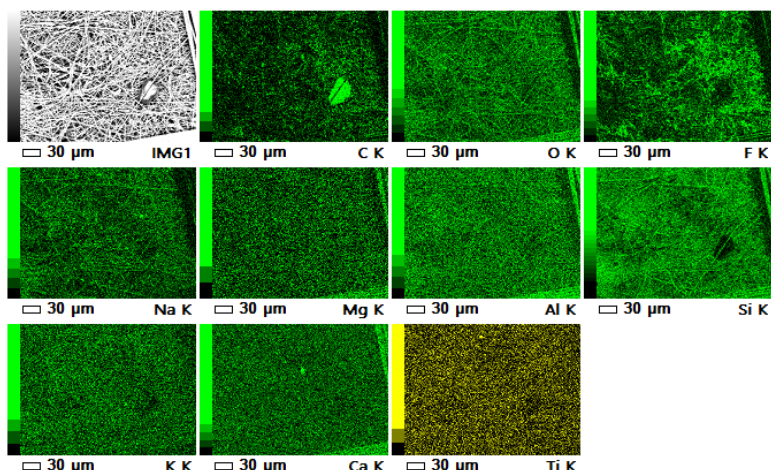


Table 11.9: EDS spectrum of NAO particles captured on the filter

11.4.2 Brake Pad Analysis

Each wheel in an automobile has one set of brake pads. The brake pads used in this experiment are floating type as explained in 5.1. Studies have shown that the type of brake pads (fixed or floating) affect the nature of wear as the brake forces acting on the disc changes with the location of the brake pad piston. The brake pads are placed on either side of the wheel, inner and outer. The inner brake pad has a retraction spring which increases the overall part thickness, while the outer one has a lower overall thickness due to the absence of the retraction spring. For the SEM and EDS analysis of the brake pad surface, the inner brake pad was chosen as it fits in perfectly into SEM chamber without damaging the electron head. In this section the change in elemental composition of the pads is compared before and after the test for different materials.

1. ECE pads with ICE cycle

Element	Mass % Before	Mass% After
C	33.88	25.78
O	10.72	6.07
Mg	4.07	1.33
Al	4.61	1.71
Si	2.06	1.02
P	0.8	0.45
S	6.4	3.83
Ca	0.65	0.3
Cr	2.35	1.28
Mn	0	0.3
Fe	10.09	50.19
Cu	1.94	1.32
Zn	7.42	2.71
Sn	9.2	3.73
Mo	5.52	0
Total	100	100

Table 11.10: Elemental composition of ECE brake pads before and after the test

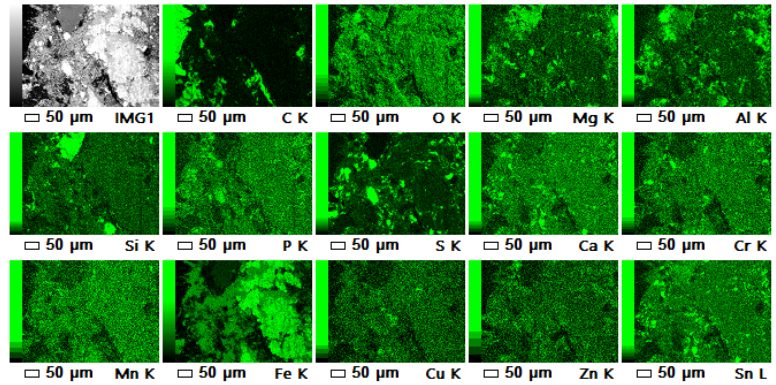


Table 11.11: Elemental composition of ECE brake pads after the test with ICE cycle

2. ECE pads with EV cycle

Element	Mass % Before	Mass % After
C	33.88	26.4
O	10.72	5.75
Mg	4.07	1.26
Al	4.61	1.18
Si	2.06	0.91
P	0.8	0.31
S	6.4	2.87
Ca	0.65	0.24
Cr	2.35	0.98
Mn	0	0.42
Fe	10.09	51.55
Cu	1.94	2.75
Zn	7.42	2.04
Sn	9.2	3.34
Mo	5.52	0
Total	100	100

Table 11.12: Elemental composition of ECE brake pads before and after the test with EV cycle

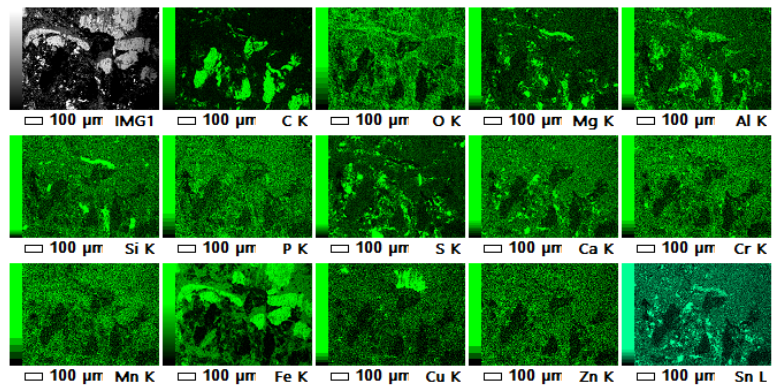


Table 11.13: EDS spectrum of ECE brake pad surface after the test

3. NAO pads with ICE cycle

Element	Mass % Before	Mass % After
C	33.17	19.27
O	10.34	14.45
Na	0.17	0
Si	2.91	3.65
S	2.25	2.09
Cl	0.95	0
K	4.96	3.41
Ca	11.66	10.43
Ti	20.27	16.12
Fe	1.71	12.06
Zn	0.25	14.14
Zr	11.36	4.38
Pt	0	4.38
Total	100	100

Table 11.14: Elemental composition of NAO brake pads before and after the test with ICE cycle

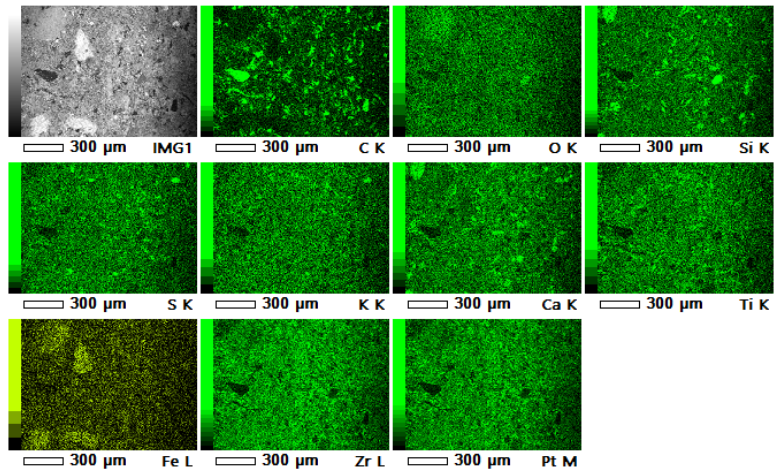


Table 11.15: EDS spectrum of NAO brake pad surface after the test

4. New NAO pads with ICE cycle

Element	Mass % Before	Mass % After
C	38.35	31.15
O	12.34	14.77
Mg	0.08	0
Si	1.96	2.41
S	2.20	2.06
K	3.04	2.24
Ca	7.86	10.79
Ti	16.05	16.76
Fe	0	6.86
Zr	11.72	12.96
Sn	6.42	0
Total	100	100

Table 11.16: Elemental composition of New NAO brake pads before and after the test with ICE cycle

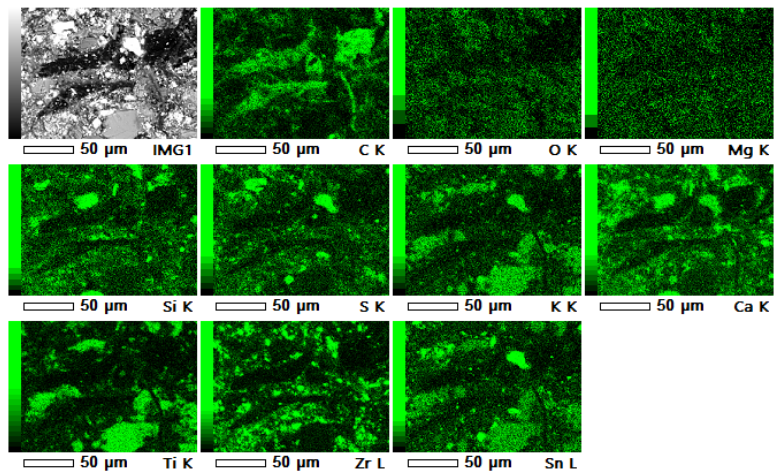


Table 11.17: EDS spectrum of New NAO brake pad surface after the test

12 Discussion

12.1 PM Emissions Comparison Between Brake Pad Materials

The mass and count distribution of different sized particles are shown in this section for each of the brake pad materials comparatively. As mentioned previously, the conventional categories for particulate matter include PM1, PM2.5, and PM10. However, in Figure 12.2, Figure 12.1, and Table 12.1 the particles will be categorized as PM1, PM1-2.5 and PM2.5-10, meaning that the PM2.5 and PM10 categories will not include all particles smaller than $2.5\mu\text{m}$ and $10\mu\text{m}$ respectively, but instead will only include the delta amount of particles between that category and the previous category. Furthermore, the values compared will be found by taking an average of the readings over the entire cycle to analyze which size of particles are most prevalent, and on average which pad materials are emitting the most particles over the course of the cycle.

Beginning with Figure 12.2 and Figure 12.1, the trend follows what was expected—that ECE on average emitted the most particles in both mass and numbers, followed by NAO and then by new NAO. However, the gap in difference ECE and NAO is larger than that of NAO and new NAO. What is particularly important to notice in these graphs is that, while the mass presence of particles above size PM1 is noticeable, the count is hardly visible in the graph. This implies that a vast majority of the particles by count are PM1 for all materials, and that larger particles are only very few but can weigh a lot comparatively to PM1.

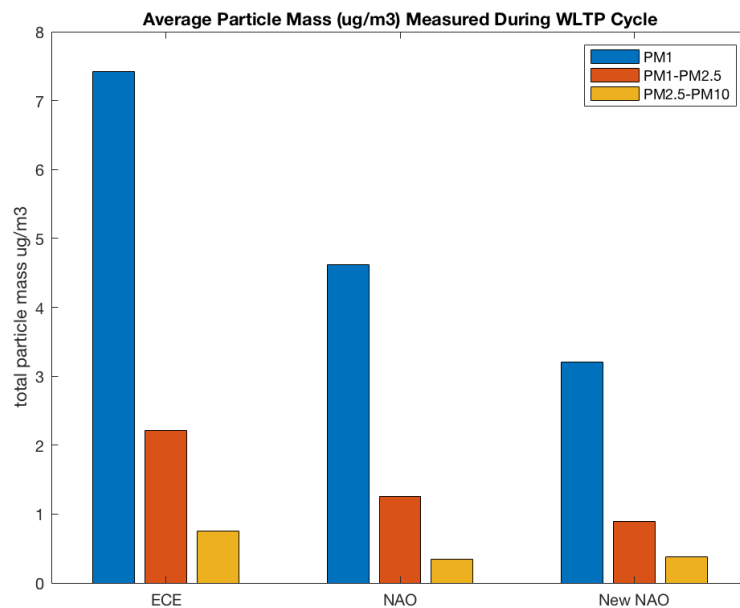


Figure 12.1: Average Particle Mass in $\mu\text{g}/\text{m}^3$ Measured During WLTP Cycle for Different Brake Pad Materials

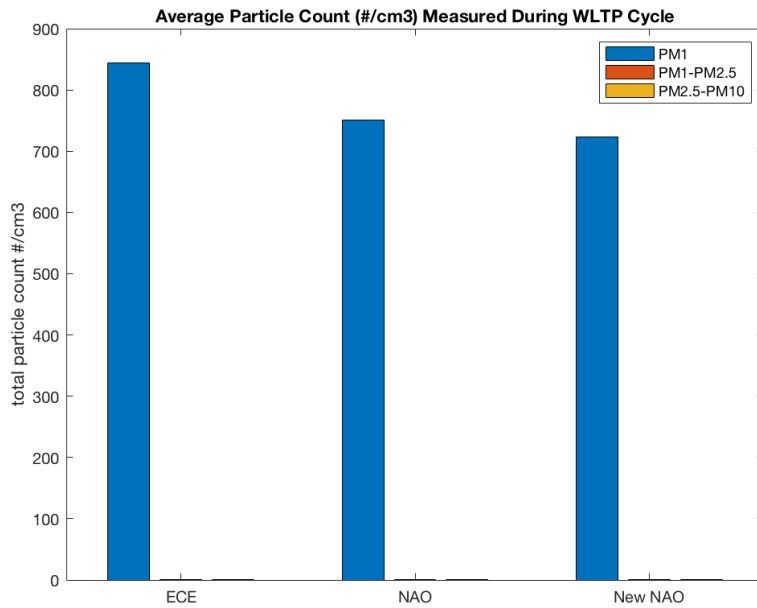


Figure 12.2: Average Particle Count in #/cm³ Measured During WLTP Cycle for Different Brake Pad Materials

Pad Material	Mass Emissions (ug/m ³)			Count Emissions (#/cm ³)		
	PM1	PM1-PM2.5	PM2.5-PM10	PM1	PM1-PM2.5	PM2.5-PM10
ECE Pads	7.427	2.214	0.754	843.788	0.713	0.014
NAO Pads	4.619	1.260	0.342	751.139	0.423	0.006
New NAO Pads	3.209	0.896	0.385	723.711	0.253	0.008

Table 12.1: Average PM Mass and Count Data for 3 Different Brake Pad Materials Over WLTP Cycle

As mentioned previously, what can be deduced from these graphs is that a vast majority of the particles present in these braking tests are particles with an aerodynamic diameter of less than 1 μm, and that switching from ECE to NAO pads will decrease the PM emissions with respect to count and mass, and switching to new NAO will even further decrease PM emissions.

12.2 PM Emissions Comparison Between Braking Cycles

This section shows the results between the ECE brake pads with the two different braking cycles– WLTP ICE cycle and EV cycle.

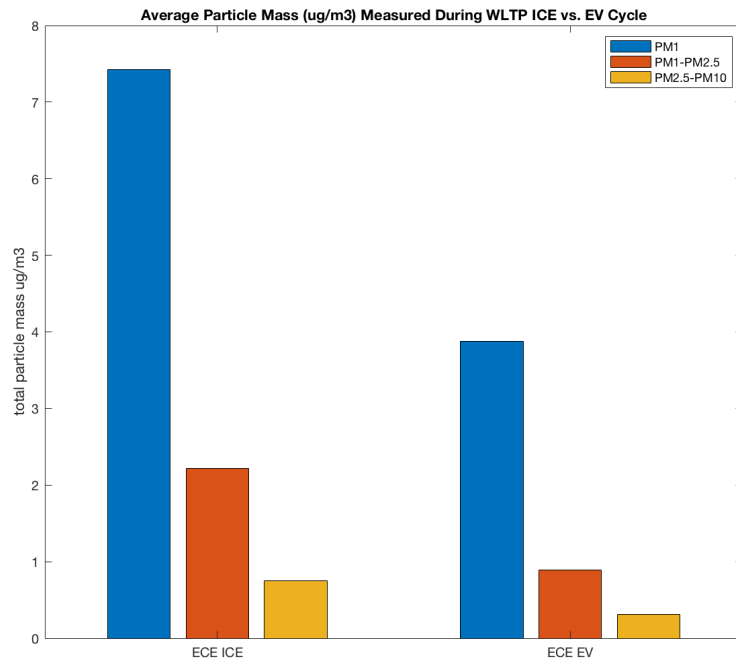


Figure 12.3: Average Particle Mass in $\mu\text{g}/\text{m}^3$ Measured During WLTP Cycle for ICE vs. EV

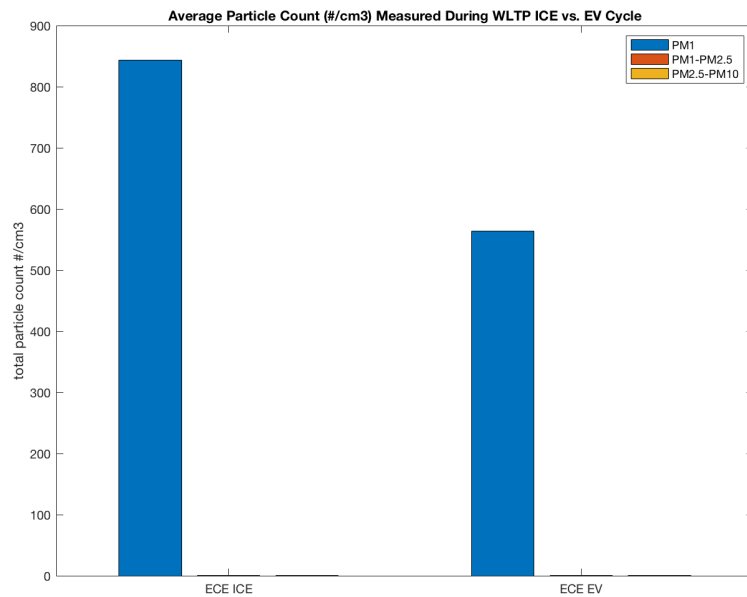


Figure 12.4: Average Particle Count in $\#/ \text{cm}^3$ Measured During WLTP Cycle for ICE vs. EV

Though the friction braking for the EV cycle is only 30% in magnitude compared to that of the ICE cycle, the difference in braking emissions is only about half by mass. Then, as mentioned above, the background noise level needs to be considered for the count emissions. From these results it is clear that switching to EVs will help to mitigate braking particle emissions.

12.3 PM Emissions Overview

These plots show an overview of the average particle measurements for the different material brake pads and two different braking cycles. The purpose of this comparison is to visualize how comparable driving an EV is to changing brake pad materials in order to decrease PM emissions from braking.

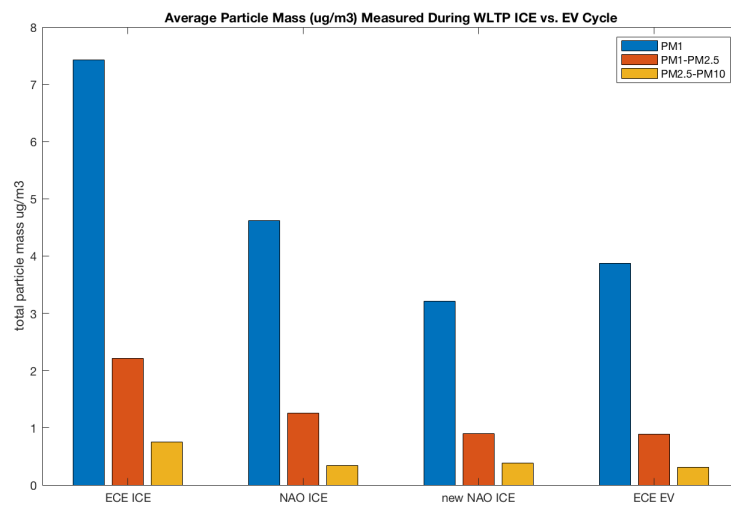


Figure 12.5: Average Particle Mass in $\mu\text{g}/\text{m}^3$ Overall Comparison Between Materials and Braking Cycles

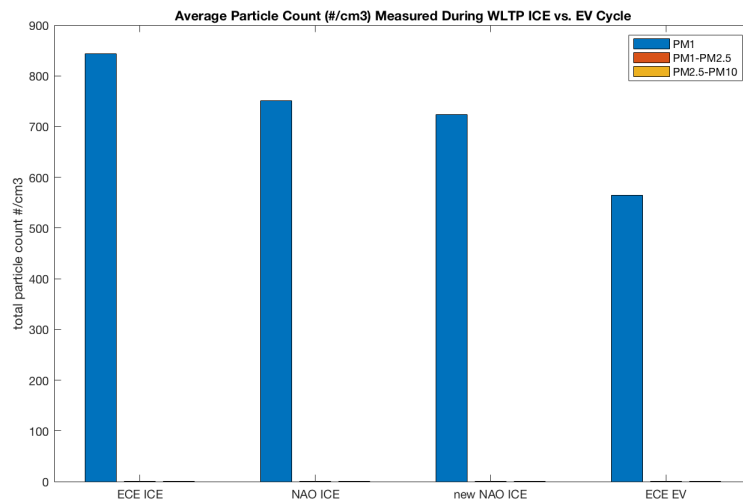


Figure 12.6: Average Particle Count in $\#/cm^3$ Overall Comparison Between Materials and Braking Cycles

Based on these plots, the conclusion drawn is that it is comparable to either switch brake pad material to "new NAO" or drive an EV in terms of emitting the least amount of braking PM. New NAO pads produce slightly less PM in terms of mass, but it shows that the EV cycle produces slightly less PM in terms of count. However, this could be due to a different background noise level in the PM count emissions.

12.4 Material Wear Comparison Between Brake Pad Materials

In this section, we will discuss about the amount of wear, nature of wear and possible improvements in the measuring methods. We will also look into the material analysis results and possible improvements in that area as well.

12.4.1 Amount of Wear

As seen in section 11.3.1, the loss of thickness and weight in the brake pads have helped us quantify material loss due to wear. Furthermore, the SEM images shed some light on the possible causes of wear.

While comparing the ECE pads against NAO pads tested with ICE cycle, for ECE pads the average decrease in thickness of the pads is 1.3% compared to 0.45% for NAO pads. A similar trend is seen in weight loss, where ECE pads have an average weight loss of 3.2% in comparison with NAO pads which have a weight loss of 0.75%. This means that the wear on ECE pads is approximately 25% more than that of NAO pads complementing the higher PM values. Although the disc material was the same in both the tests, the disc thickness decrease with ECE pads was approximately 15% more than that with NAO pads suggesting that the pad material influences the amount of wear on the discs. As per theory [23], we know that amount of wear is dependent on the ability of the friction material to form the friction layer. In case of ECE, the failure of higher amounts of steel fibers

create a lot of wear debris which influences the growth of secondary plateau. The tendency of secondary plateau formation usually indicates highest wear [34].

SEM images confirm the adhesive friction of pads, failure of secondary plateaus which are the root cause of wear and in turn PM emission.

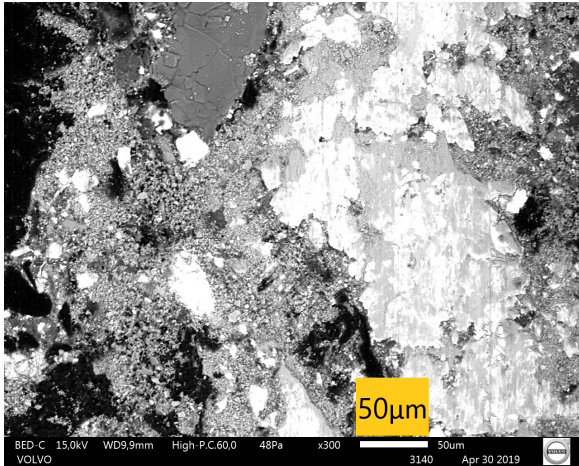


Figure 12.7: Adhesive friction on ECE pads (ICE cycle)

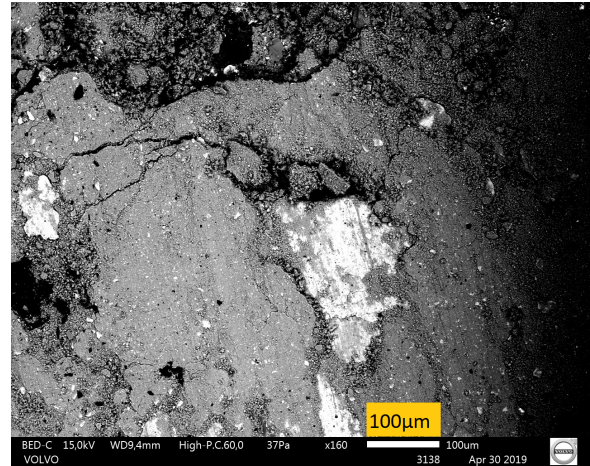


Figure 12.8: Secondary plateau failure in ECE pads (EV cycle)

However, it is interesting to see that there is an increase in disc weight after test 8 (ECE pads tested with WLTP EV). The reason for mass gain could be that the material loss due to wear is less than the material gain by corrosion layer built up over 2 days. This is complementary to the reduced PM emissions during test 8 compared to other tests. While one can be happy about the reduced emission, there could be a possibility that the disc weight is constantly increasing during an EV braking cycle as cast iron has a higher corrosion rate.

12.4.2 Nature of Wear

Studies have shown that the wear pattern depends on the type of brake pads used (floating or fixed type) as the forces acting on the brake pads in each case are different [35]. The brake pads used in our tests are floating type. So, the inner pads have a single piston located at the center of the pad while the outer piston has two pistons located on the two ends as shown in the figure below

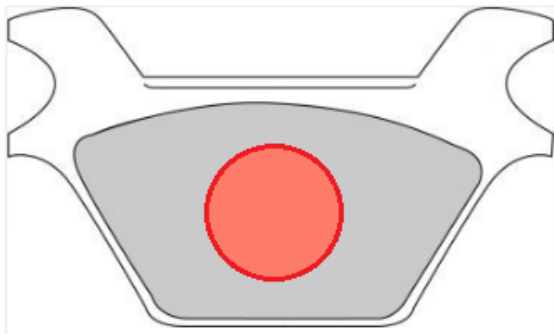


Figure 12.9: Piston location on inner pads

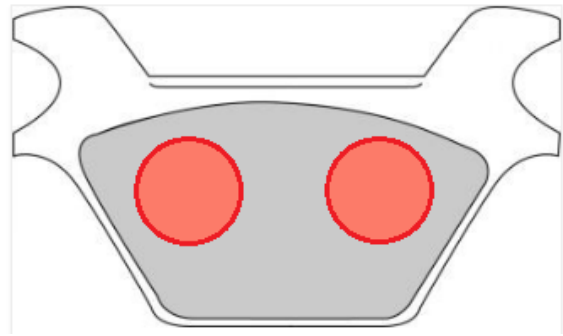


Figure 12.10: Piston location on outer pads)

By looking at the flatness profile measurements 11.3.2 of different brake pad materials, we can notice two distinct patterns of wear:

1. The amount of wear is more on the ends of the outer pads. This means that wear is probably happening at the location where the piston contact is happening resulting in a convex brake pad surface
2. At the inner pads, since we have one piston located centrally, the wear must happen centrally creating a concave surface. But, the brake pad surface is almost flat. This can probably mean that the piston in the inner pads much larger than that of outer pads resulting in a uniform wear pattern

These are important observations which are in line with the simulation studies which infer that in a single-piston type brake pad, contact pressure and resulting wear at the pad midpoints is higher [35]. Simulation studies also state that the amount of wear in a double-piston is less than that in a single-piston type of caliper when the piston contact area in both the cases are the same i.e. the combined piston surface area of two pistons in a double-piston type of caliper should be equal to piston surface area of the single-piston type. This is not inline with our results which show that the inner pad (single-piston type) has less wear compared to outer pad (double-piston type) which may signify that the piston contact areas in both cases may not be equal.

Further, the surface roughness measurements suggest that the surface roughness on the NAO and the New NAO pads decrease drastically compared to the ECE pads. The variation in the surface roughness parameters is shown in the figure below.

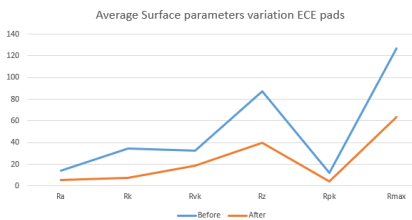


Figure 12.11: ECE pads

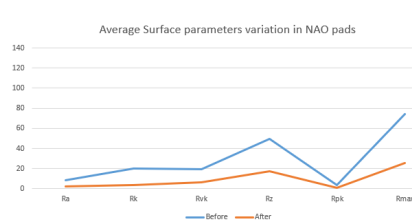


Figure 12.12: NAO pads

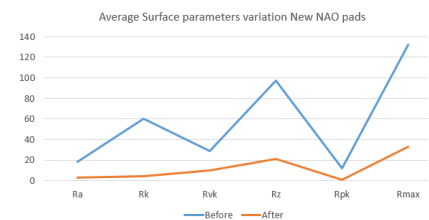


Figure 12.13: New NAO pads

One of the important properties for friction material is the ability to provide constant coefficient of friction throughout and this depends on the surface roughness and hardness [20] of the brake pad surface. Since, the surface roughness directly impacts the brake squeal performance [36], ECE and NAO pads might give better brake squeal performance compared to New NAO pads but that comes with higher PM emissions. To have a strong inference regarding this, the accuracy of the measurements needs to be improved. This can be done by:

1. Increasing the sample size to 100 points from current size of 5 points by using a 3D profilometer which measures 100 points in a couple of minutes. A sample measurement was done using 3D profilometer at RISE IVF which not only measures the roughness parameters but also gives the 3D image of the surface topography as shown in the figure

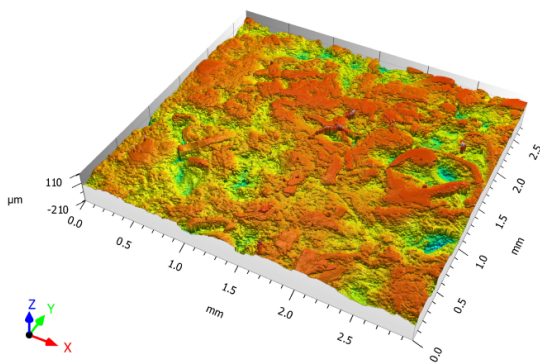


Figure 12.14: 3D surface topography of new ECE pad

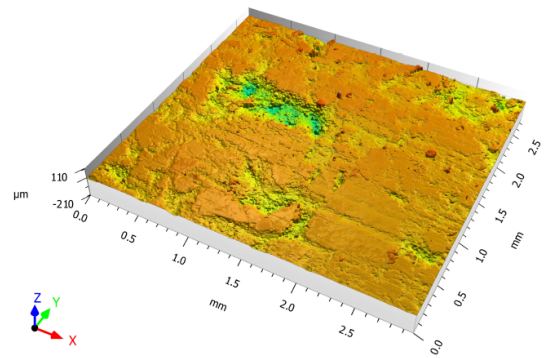


Figure 12.15: 3D surface topography of worn ECE pad

2. Measuring the roughness vertically instead of horizontally. As seen in the 3D profilometry image, there are a lot of grooves formed along the sliding direction. So, it is better to measure the roughness in a direction perpendicular to the sliding direction as shown in the figure below

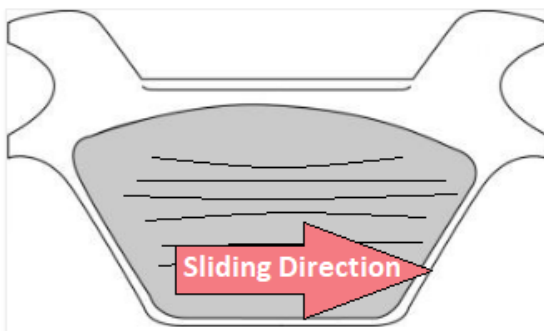


Figure 12.16: Sliding direction on the pad

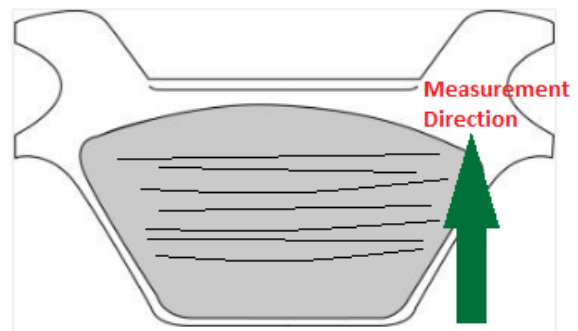


Figure 12.17: Measuring direction on the pad

12.4.3 Elemental Analysis of Brake Pad Surface

The main purpose of conducting the EDS analysis of particles and the brake pad surface was to understand if any elements, toxic to human health are present. Analysis of brake pad particles collected by the filter would have served the purpose, but as discussed in 11.4.1 we were not satisfied by the results. So, the next best thing was to analyse the brake pad surface and find out if it had any harmful particles, since the airborne particles are of course derived from the elements on the surface. By referring to section 6.1, we know the elements which are harmful to human health with some short term and long term effects.

The EDS analysis results 11.4.2 show that ECE pads may have harmful elements like Mg, Al, Cr, Cu, and Zn. One of the notable change in mass percentage is with respect to Fe. During both ICE and EV cycle there is an increase in Fe mass percentage on the pads after the experiment five fold. This acts as an evidence to show that adhesive friction can be a possibility.

The NAO pads are less harmful compared to ECE pads with possible toxic elements like Ca, Ti, and Pt. The presence of platinum is however doubtful when we consider its cost and availability in nature. As far as the application in friction materials is concerned, Platinum is used in race cars as it provides linear and consistent co-efficient of friction resulting in incredible feedback and control as claimed by a premium brake pad manufacturer. It might also be possible that Pt is found because of some overlapping spectrum.

The safest among the three candidates is the New NAO pads which do not show presence of any harmful contents. The adhesive friction is the however seen in both NAO and New NAO. Since the EDS analysis is only done on certain locations of the pad, there is a possibility that some additional elements might be discovered.

12.5 Best Brake Pad Candidate for Reduced Environmental and Human Impact

When we look at the PM emission data, we can see that the New NAO pads have the least amount of emission. Further, from the EDS analysis backed with some studies, we may say that the elements present in new NAO pads are much safer compared to NAO or ECE.



13 Conclusion

The main purpose of this thesis was to come up with a methodology to measure and analyse brake particles emission in order to understand the environment and health impacts of the same. Three different sets of brake pads were tested with 2 different cycles. Further, nature of wear on these brake pads is studied so that it acts as an input while making any design changes in the future. With the current test set up we can say that New NAO pad produces the least PM emission compared to the ECE and NAO pads.

Even though the brake PM collection was done using a filter, the efficiency of collection needs to be improved without affecting the air flow in the test rig. The same applies to the PM analysis from the filter as the filter was polymer based and there was difficulty analysing it using SEM and EDS. The best way to understand the elements of a brake pad was to do an EDS analysis on the 3 locations of pad surface. After comparing the analysis results with literature, we may conclude New NAO pads are much safer compared to ECE with absence of harmful elements like Copper. The studies conducted in this thesis found that semi-metallic brake pads produced the most emissions in both mass and count, while the new non-asbestos organic brake pads produced the least emissions, and also contained the least harmful elemental components in the particles created from abrasion.

Comparison between EV cycle and ICE cycle with regards to PM emission shows that the WLTP EV cycle produces less particles in terms of both number and mass distribution. This is attributed to regenerative braking which in turn affects the overall braking energy requirements on friction braking.

Considering the current braking emissions with WLTP ICE cycle and ECE brake pads in Europe, PM emissions in the future can be reduced by adopting better brake pad material or going electric. While comparison between PM emissions in New NAO pads and WLTP EV cycle suggest that New NAO pads produce lower PM mass compared to WLTP EV cycle. But, its vice versa when it comes to PM count. So, looking at the results we have from this study it can be inferred that either changing the brake pad material or drive cycle can result in drop in PM emissions from current levels.

If either of the above solutions are difficult to implement, then brake particles can be filtered out when they are emitted from the vehicle. Since the amount and nature of wear is dependent on the number of contact points on the brake pads, brake pad design can be changed based on the contact point. This may not only reduce wear but also change the wear pattern which is important to be assessed when designing a brake filter in the future.

In short, this thesis has developed a testing procedure for measuring braking emissions created during an average, everyday driving cycle. A correlation between the particulate matter emissions and disc temperature, braking energy, and speed of the vehicle during braking was found and some trends found in these experiments were confirmed with previous studies. Of the three materials studied in this thesis, the use of new non-asbestos organic brake pads is recommended in order to decrease the quantity of emissions caused by braking as much as possible, as well as reduce the risk to human health posed by particulate matter of dangerous elemental compounds.



14 Future Work & Recommendations

- Corrosion tests should be run again for the ECE and NAO pads, without running the burnishing cycle beforehand.
- Several tests should be carried in the brake dynamometer with the same chamber air speed (40 kph) and without braking events, in order to determine the background noise of particles.
- The instrumentation for measuring and collecting the particles needs to be improved. A direct low pressure impactor might be a good choice as it will have a higher sampling frequency for particle measurement in addition to collecting them for further chemical analysis.
- In the event of continuing with the electrostatic precipitator particle measurement in the future, a multistage HEPA filter can be used to collect the particles and then use thermogravimetric analysis for the chemical analysis of particles.
- Aluminum brake discs and their corresponding pads were ordered to be tested in this thesis, but unfortunately the discs could not be mounted to the brake dynamometer since the rig has not tested these discs before and therefore did not have the proper attachment on hand. However, this material would be interesting to test in comparison to the other materials with gray cast iron discs to see what the difference with respect to PM emissions would be. Furthermore, these discs could also be tested with the EV cycle since the operating temperatures and brake energy required for friction braking in EVs are less, and since aluminum discs have a lower heat capacity than gray cast iron discs, they would be suitable for this application in order to reduce weight.
- Atmospheric brake PM emissions can be reduced by:
 1. Incorporating a filter in the vehicle which collects particles as they are emitted.
 2. Changing the material composition and design of friction materials.
 3. Replacing ICE vehicles on the road with hybrids or EVs.

References

- [1] Mathworks. Disc brake, 2019. [4](#), [8](#)
- [2] Carbiketech.com. What is regenerative braking in cars & how does it work?, 2019. [4](#), [10](#)
- [3] United Nations Economic Commission for Europe. Particle measurement program 47th session, 2018. [4](#), [16](#), [17](#), [18](#)
- [4] Air Quality Team. Call for evidence on brake, tyre and road surface wear, 2018. [4](#), [19](#), [20](#)
- [5] Jennifer MacDonald. Electric vehicles to be 35% of global new car sales by 2040. *Bloomberg New Energy Finance*, 25, 2016. [4](#), [20](#), [21](#)
- [6] F. Amato. *Non-Exhaust Emissions: An Urban Air Quality Problem for Public Health; Impact and Mitigation Measures*. Elsevier Science, 2018. [7](#), [11](#), [12](#), [13](#), [14](#), [27](#), [28](#), [31](#), [47](#)
- [7] World Health Organization. Health and sustainable development - air pollution, 2019. [7](#)
- [8] Till Bunsen, Pierpaolo Cazzola, Marine Gorner, Leonardo Paoli, Sacha Scheffer, Renske Schuitmaker, Jacopo Tattini, and Jacob Teter. Global ev outlook 2018: Towards cross-modal electrification. 2018. [7](#), [16](#), [20](#)
- [9] Paul G Sanders, TM Dalka, N Xu, M Matti Maricq, and RH Basch. Brake dynamometer measurement of airborne brake wear debris. *SAE Transactions*, pages 1693–1699, 2002. [9](#)
- [10] Environmental Protection Agency. Health and environmental effects of particulate matter (pm), 2018. [11](#), [14](#)
- [11] Rebrake. Rebrake, 2017. [13](#)
- [12] EU Publications Office. European commission cordis, 2017. [13](#)
- [13] Bhagwan D Garg, Steven H Cadle, Patricia A Mulawa, Peter J Groblicki, Chris Laroo, and Graham A Parr. Brake wear particulate matter emissions. *Environmental Science & Technology*, 34(21):4463–4469, 2000. [14](#), [17](#), [43](#)
- [14] Paul G Sanders, Ning Xu, Tom M Dalka, and M Matti Maricq. Airborne brake wear debris: size distributions, composition, and a comparison of dynamometer and vehicle tests. *Environmental science & technology*, 37(18):4060–4069, 2003. [15](#)
- [15] Hiroyuki Hagino, Motoaki Oyama, and Sousuke Sasaki. Laboratory testing of airborne brake wear particle emissions using a dynamometer system under urban city driving cycles. *Atmospheric Environment*, 131:269–278, 2016. [15](#), [47](#)
- [16] Akihiro Iijima, Keiichi Sato, Kiyoko Yano, Hiroshi Tago, Masahiko Kato, Hirokazu Kimura, and Naoki Furuta. Particle size and composition distribution analysis of automotive brake abrasion dusts for the evaluation of antimony sources of airborne particulate matter. *Atmospheric Environment*, 41(23):4908–4919, 2007. [15](#)
- [17] Scott Shepard and Lisa Jerram. Transportation forecast: Light duty vehicles. *Boulder, CO: Navigant Consulting, Inc*, 2015. [20](#)



- [18] Peter J Blau. Compositions, functions, and testing of friction brake materials and their additives; topical. Technical report, Oak Ridge National Lab., 2001. [22](#), [23](#), [24](#), [25](#), [26](#)
- [19] Umberto Paolo Passarelli, Fabrizio Merlo, Diego Pellerej, and Pietro Buonficio. Influence of brake pad porosity and hydrophilicity on stiction by corrosion of friction material against gray cast iron rotor. Technical report, SAE Technical Paper, 2012. [22](#), [23](#)
- [20] KL Sundarkrishnaa. Design essentials—friction material composite system. In *Friction Material Composites*, pages 75–98. Springer, 2015. [23](#), [24](#), [59](#)
- [21] Jie Fei, Wei Luo, Jian Feng Huang, HaiBo Ouyang, ZhanWei Xu, and ChunYan Yao. Effect of carbon fiber content on the friction and wear performance of paper-based friction materials. *Tribology International*, 87:91–97, 2015. [24](#)
- [22] Ho Jang and Seong Jin Kim. The effects of antimony trisulfide (sb₂s₃) and zirconium silicate (zrsio₄) in the automotive brake friction material on friction characteristics. *Wear*, 239(2):229–236, 2000. [25](#)
- [23] Mikael Eriksson and Staffan Jacobson. Tribological surfaces of organic brake pads. *Tribology international*, 33(12):817–827, 2000. [25](#), [31](#), [32](#), [56](#)
- [24] Luise Gudmand-Høyer, Allan Bach, Georg T Nielsen, and Per Morgen. Tribological properties of automotive disc brakes with solid lubricants. *Wear*, 232(2):168–175, 1999. [25](#)
- [25] Yuji Handa and Takahisa Kato. Effects of cu powder, baso₄ and cashew dust on the wear and friction characteristics of automotive brake pads. *Tribology Transactions*, 39(2):346–353, 1996. [25](#)
- [26] G Nicholson. Facts about friction. croydon, pa: P&w price enterprises, 1995. [26](#)
- [27] HD Bush, DM Rowson, and SE Warren. The application of neutron activation analysis to the measurement of the wear of a friction material. *Wear*, 20(2):211–225, 1972. [26](#)
- [28] Omar Maluf, Maurício Angeloni, Marcelo Tadeu Milan, Dirceu Spinelli, and Waldek Wladimir Bose Filho. Development of materials for automotive disc brakes. *Minerva*, 4(2):149–158, 2007. [26](#), [27](#), [28](#)
- [29] Koji Kato and Koshi Adachi. Wear of advanced ceramics. *Wear*, 253(11-12):1097–1104, 2002. [30](#)
- [30] TR Chapman, DE Niesz, RT Fox, and T Fawcett. Wear-resistant aluminum–boron–carbide cermets for automotive brake applications. *Wear*, 236(1-2):81–87, 1999. [30](#)
- [31] L Gorjan, M Boretius, G Blugan, F Gili, D Mangherini, X Lizarralde, M Ferraris, T Graule, A Igartua, G Mendoza, et al. Ceramic protection plates brazed to aluminum brake discs. *Ceramics International*, 42(14):15739–15746, 2016. [30](#)
- [32] Mikael Eriksson, John Lord, and Staffan Jacobson. Wear and contact conditions of brake pads: dynamical in situ studies of pad on glass. *Wear*, 249(3-4):272–278, 2001. [32](#)
- [33] Marcel Mathissen, Jaroslaw Grochowicz, Christian Schmidt, Rainer Vogt, Ferdinand H Farwick zum Hagen, Tomasz Grabiec, Heinz Steven, and Theodoros Grigoratos. A novel real-world braking cycle for studying brake wear particle emissions. *Wear*, 414:219–226, 2018. [37](#)
- [34] Jayashree Bijwe and Mukesh Kumar. Optimization of steel wool contents in non-asbestos organic (nao) friction composites for best combination of thermal conductivity and tribo-performance. *Wear*, 263(7-12):1243–1248, 2007. [57](#)



- [35] Amirhossein Hatam and Abolfazl Khalkhali. Simulation and sensitivity analysis of wear on the automotive brake pad. *Simulation Modelling Practice and Theory*, 84:106–123, 2018. [57](#), [58](#)
- [36] M Kchaou, AR Mat Lazim, AR Abu Bakar, J Fajoui, R Elleuch, and F Jacquemin. Effects of steel fibers and surface roughness on squealing behavior of friction materials. *Transactions of the Indian Institute of Metals*, 69(6):1277–1287, 2016. [59](#)

